IEEE Access
Multidisciplinary | Rapid Review | Open Access Journal

Received 29 April 2023, accepted 24 May 2023, date of publication 2 June 2023, date of current version 12 June 2023.

Digital Object Identifier 10.1109/ACCESS.2023.3282178

RESEARCH ARTICLE

Theory of Broadband Noise Matching for HF/VHF Receivers With Electrically Small Antennas

YUANXUN ETHAN WANG, (Fellow, IEEE)
Electrical and Computer Engineering Department, University of California, Los Angeles, CA 90095, USA
e-mail: ywang@ee.ucla.edu

This work was supported in part by the Office of the Director of National Intelligence (ODNI), Intelligence Advanced Research Projects Activity (IARPA), under Grant 2021-2106240007.

ABSTRACT A general theory on noise matching performance of receivers with electrically small antennas (ESAs) emphasizing HF (3MHz to 30MHz) and VHF (30MHz to 300MHz) applications is presented through theoretical analyses, discussions, and circuit simulations with practical device models from a state-of-the art semiconductor technology. The theory considers all the noise sources and their interplay. The impact on the noise performance from both the physical constraint of the ESA in terms of its radiation quality factor and the scaling of transistor technology and periphery such as gate resistance, gate cutoff frequency and transition frequency has been discussed. Two receiver examples, one with electrically small dipole and the other with electrically small loop are studied with full-wave simulations. The antenna equivalent models are then connected to low noise amplifiers designed with the state-of-the-art Gallium Nitride (GaN) transistor models to evaluate the noise performance of the systems and compared against the theory. It is demonstrated that both the noise figure and its bandwidth can be significantly improved over traditional matching strategy when optimized active direct matching is applied at the price of increased device periphery and power consumption. In particular, the bandwidth of such low noise matching can be orders of magnitude wider than the antenna's conjugate impedance matching bandwidth that is defined by Harrington-Chu's limit.

INDEX TERMS Broadband matching, electrically small antennas, GaN transistors, HF antennas, low noise matching, receivers, VHF antennas.

I. INTRODUCTION

Wireless communications in high frequency (HF) band (3MHz to 30MHz) and very high frequency (VHF) band (30MHz to 300MHz) are of particular interest as electromagnetic waves in these bands can propagate for a long distance through ionosphere reflections or diffractions and penetrate well through buildings and foliage. One challenge associated with these systems is that the antenna sizes at resonant dimensions may become impractically large. Electrically small antennas with self-resonant or external matching networks can be used for receivers at these frequencies [1], [2], [3], [4], [5], [6], [7], [8], [9], [10] yet the sensitivities and operation bandwidth are often limited.

The associate editor coordinating the review of this manuscript and approving it for publication was Abhishek K. Jha.

Traditionally antenna matching to a receiver is carried out as two separate tasks. A common interface impedance, e.g., 50Ohm, is often set at first so that the antenna output is conjugately matched to this common impedance through a matching network. On the other hand, the input of a low noise amplifier (LNA) as the first stage of the receiver is also designed to noise match to this common impedance. Noise matching means a minimum noise figure of the LNA is yielded at this source impedance while the value of the impedance may often be far off from that in the conventional conjugate match condition. This strategy guarantees the best signal to noise ratio (SNR) of the receiver system for a given low noise amplifier and for signal within the matched bandwidth when the loss of the antenna matching network is not considered.

However, several shortfalls may occur when this matching strategy is applied to HF/VHF receivers with electrically

small antennas (ESAs). First, the radiation resistances of are often very small with sub-Ohm values. Transforming thses extremely low radiation resistances to 50Ohm will inevitably incur great loss with any standard impedance matching network. Same may be applied for the impedance transformation network between the LNA and the common impedance interface, particularly when low quality factor inductors are used as part of the matching networks. The loss in the matching network may elevate the noise level in the receiver and defeat any benefit harvested from the noise matching. Second, even with a noiseless assumption, a matching network often yields the desired impedance only over a small fraction of the bandwidth which may cause the noise figure of the receiver quickly rise up outside the matched bandwidth. The high radiation quality factor of an ESA [11], [12], [13] also implies an inherently narrow impedance matching bandwidth as defined by the Bode-Fano limit. Third, state-of-the-art transistors offer exceptionally high gain and low noise at HF/VHF frequencies which may allow more design space for a LNA to trade off its gain for noise matching performance. This also means the connected antenna may operate further away from the conventional conjugate matching condition for noise benefits. Yet the selection of transistors and the design of LNA are traditionally done separately without considering the impact of the ESA thus the benefit of joint design is not utilized toward the maximum noise matching performance of the receiver.

On the other hand, active matching networks for antennas with transistors or parametric amplifiers have been attempted by many since 1960s [14], [15], [16], [17], [18], [19], [20]. The noise performance of directly connecting electrically small antennas to an amplifier, whether it is a Bipolar transistor (BJT), Field effect transistor (FET) or a parametric amplifier have been analyzed since 1965 [21]. Unfortunately, neither those experiments or analyses led to insights on how such receivers should be designed toward the best noise and bandwidth performance that are comparable or even superior to the traditional impedance matched designs. Non-foster matching techniques based on negative impedance converters (NIC) have also been proposed and studied [22], [23], [24], yet it has been concluded in [24] that this technique does not offer system advantages in terms of noise figure, largely due to the added noise of the NIC circuit. Recently, several experimental works [25], [26], [27], [28] demonstrated that traditional matching strategies of ESAs did not result better signal to noise performance or better noise bandwidth in experiments comparing with direct connection of ESAs to a buffer amplifier [25], an op-amp [26] or parametric amplifiers [27], [28]. These findings call for a re-evaluation of the noise matching strategy for receivers with electrically small antennas, particularly given the fact that active electronics has undoubtfully improved significantly over the past half a century.

The objective of this paper is to develop a general theory on noise matching performance of receivers with ESAs through theoretical analyses and discussions, and circuit simulations with practical device models from a state-of-the art semiconductor technology. Such a theory has been largely missing from the existing literatures to the best knowledge of the author. Some existing theoretical treatments of noise contribution of amplifiers in the antenna system are based on a constant LNA noise figure assumption which implies a constant amount of noise power is added in the receiver front-end [25], [27], [29] while in reality the amount of the noise added by the front-end is significantly impacted by the antenna's own impedance. Other classical treatments of transistor noises use an optimum noise impedance formulation derived from equivalent voltage and current noise sources observed through measurements [21]. However, the formulation has neither linked to the known scalable physical parameters of transistors such as gate periphery and transition frequencies, nor considered the practical constraints of the ESA impedance such as those imposed by Harrington-Chu's limit or Gustafsson's limit [11], [12], [13]. In this paper, a unified theoretical framework considering all the noise sources and their interplay is proposed. The impact on the noise performance resulting from both the physical constraint of the ESA in terms of its radiation quality factor and the scaling of transistor technology and periphery such as gate resistance, gate cutoff frequency and transistor transition frequency has been discussed. It shows an optimized strategy of matching low noise transistors to ESAs directly often lead to much superior noise figure and over a much broader bandwidth comparing to the traditional matching strategy. The theory also provides guidance on how to optimize the periphery of the transistors for a given ESA toward the best noise performance of the receiver.

The paper is organized as follows. First, the noise performance of the receiver is formulated by using a noise figure defined from the wave port of the ESA to the output of the detector. This metrics includes the impact of both the antenna noise due to its finite radiation efficiency and the noise added by the detector which is often an amplifier consisting of transistors or varactor diodes. For this purpose, equivalent circuit models of ESAs are derived and coupled to that of the transistors so that the impact on the noise performance by both parties can be clearly identified. Second, based on the understanding of the interplay between the noise and impedance matching, several strategies of matching the antenna to the detector as well as the optimization of the transistor detector peripheries are proposed. These design options result in either an optimum noise figure with a maximum bandwidth or low power consumption. To validate the proposed noise matching theory and to demonstrate the efficacy of the proposed matching strategy, two receiver examples, one with an electrically small dipole and the other with an electrically small loop, are studied through full-wave and circuit simulations. Both antennas are with the maximum electrical dimensions of ($ka = 1/4$) at 100MHz and connected with LNAs designed with state-of-the-art GaN transistors offered by Hughes

Research Laboratory (HRL). The noise figures of receivers are evaluated with the foundry provided device models under different matching conditions and compared with the analytical predictions of the proposed theory. It will be shown through the appropriate co-design of LNA and ESA, both the noise figure and noise matching bandwidth can be significantly improved over the conventional impedance matched case. In particular, the bandwidth of such low noise matching can be orders of magnitude higher than the antenna's conjugate impedance matching bandwidth that are defined by Harrington-Chu's limit.

II. EQUIVALENT CIRCUIR MODELS FOR ESAS

Equivalent circuit models for ESAs have been well discussed in several textbooks [30]. Here some of these discussions are recaptured here for two purposes. The first objective is to analytically express the inherent dispersive nature of the ESA radiation over a broad bandwidth. The second objective is to establish a feasible approach for analyses and simulations of the receiver gain and noise figure that is defined from the wave port of the antenna to the output of the LNA. This is necessary as most commercial full-wave simulation software for antennas can only simulate the radiation efficiency and S-parameters of the antenna in transmitting mode and the noise figure of the antenna is often derived by applying reciprocity. Here it is not possible to derive the receiver gain and noise figure without an explicitly defined wave port as the nonreciprocity no longer holds when active electronics exists. For this reason, we will first extract an explicit circuit model from the S-parameters obtained from full-wave simulations so that signal sources, noise sources and source resistances can all be clearly defined for system performance analyses.

A series resistor-capacitor model for electrically small dipole and a series resistor-inductor model for electrically small loops are often quoted in textbooks [30]. Yet more accurate circuit models that represent the broadband behavior of ESAs were presented in Chu's original paper [12] where the famous Chu's limit was derived. Chu's circuit models for the lowest order electric dipole (TM_1) and magnetic dipole mode (TE_1) are shown in the middle row of Fig.1(a) and (b), which were intended to represent the near field energy characteristics of both modes outside a sphere of radius a that encloses the antenna. The following values of the inductance and capacitance relating to its radiation resistance R_r are specified,

$$\begin{cases} L_0 = \dfrac{a}{c} R_r \\ C_0 = \dfrac{a}{c}\dfrac{1}{R_r} \end{cases} \tag{1}$$

where c is the free space speed of light. By using a different set of L_0 and C_0 parameters, the circuit models presented in Fig.1 have been found to be good representations of broadband behaviors of electrically small dipoles or loops in general [31] as the parameters L_0, C_0 and R_r remain almost frequency independent from the DC to the antenna's first

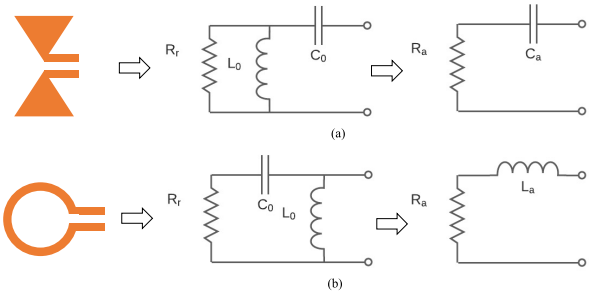

FIGURE 1. (a) Electrically small dipole (left) represented by an equivalent circuit model (middle) that assumes TM_1 mode in Chu's paper [12] or a simplified series resistor capacitor model (right) often quoted in the textbooks. (b) Electrically small loop (left) represented by an equivalent circuit model (middle) that assumes TE_1 mode in Chu's paper [12] or a simplified series resistor inductor model (right) often quoted in textbooks.

resonance frequency. Under the high-Q assumptions, either of Chu's circuit models can be simplified to a series of only two components as shown in the rightmost row of Fig.1(a)(b) through the following relation,

$$\begin{cases} R_a \approx \dfrac{(\omega L_0)^2}{R_r}, & C_a \approx \dfrac{C_0}{1-\omega^2 L_0 C_0} \approx C_0 \\ \quad (\textit{electrically small dipole}) & \\ R_a \approx \omega^4 L_0^2 C_0^2 R_r, & L_a \approx \dfrac{L_0}{1-\omega^2 L_0 C_0} \approx L_0 \\ \quad (\textit{electrically small loop}) & \end{cases} \tag{2}$$

It should be noted that the models in (2) give a capacitance and an inductance that are approximately constant only when the operating frequency is much below the first resonance of the antenna, yet the radiation resistances are now proportional to the second order and the fourth order of the frequency respectively. The radiation quality factors are given by,

$$\begin{cases} Q_a = \dfrac{1}{\omega C_a R_a} \approx \dfrac{R_r}{\omega^3 L_0^2 C_0} \\ \quad (\textit{electrically small dipole}) \\ Q_a = \dfrac{\omega L_a}{R_a} = \dfrac{\omega L_0}{\omega^4 L_0^2 C_0^2 R_r} \approx \dfrac{1}{\omega^3 L_0 C_0^2 R_r} \\ \quad (\textit{electrically small loop}) \end{cases} \tag{3}$$

Both radiation quality factors are inversely proportional to the cubic order of the operating frequency, which is consistent to what were stated in Chu's limit [12]. For convenience of discussions in the later sections, one may define the antenna's transition frequency as the frequency when the quality factors in (3) reduce to 1, i.e.

$$\begin{cases} \omega_{at} = \sqrt[3]{\dfrac{R_r}{L_0^2 C_0}}, & Q_a = \dfrac{\omega_{at}^3}{\omega^3} \\ \quad (\textit{electrically small dipole}) & \\ \omega_{at} = \sqrt[3]{\dfrac{1}{L_0 C_0^2 R_r}}, & Q_a = \dfrac{\omega_{at}^3}{\omega^3} \\ \quad (\textit{electrically small loop}) & \end{cases} \tag{4}$$

It is also evident from (2) that the radiation resistance of electrically small loop is much smaller than that of electrically small dipole for lower frequency, i.e., very small ka values. A loop of multiple turns is often used to boost up the radiation resistance, yet the Ohmic resistance of the loop itself cannot be ignored, which may add noise to the antenna and set its sensitivity limit [25]. On the other hand, the radiation of electrically small dipole is relatively more efficient and impact of the Ohmic resistance is less as a larger conductor cross-section and shorter current flow path is often available in dipole structures.

III. NOISE THEORY OF ESA

A. SIGNAL TO NOISE (SNR) PERFORMANCE OF ESA WITH NOISELESS DETECTORS

The primary noise sources for antennas in the HF/VHF bands include the background or environment noise received by the antenna, the thermal noise added by the antenna due to the existence of the loss in the antenna and the thermal noise added by the loss of the matching network if a matching network is used. The background noise of the antenna originated from various sources of radiation in the environment could be 20 to 40dB higher than thermal radiation [25] at HF but gradually approach to the same level as the thermal radiation for VHF. To simplify the noise discussion here, thermal equilibrium is assumed, i.e., the environment and the physical structure of the antenna and the matching network are all in room temperature and only thermal radiation is considered as background noise. A higher background noise can be included later once the noise performance of the receiver is determined under this thermal equilibrium condition.

For most ESAs such as electrically small dipoles and loops, an equivalent circuit model representing the operation of the receiving antenna and various noise sources are depicted in Fig.2.

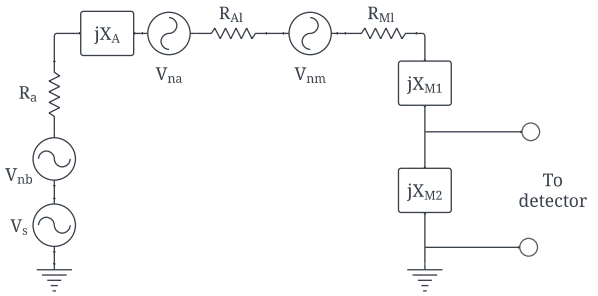

FIGURE 2. Equivalent circuit model of a receiving ESA and various noise sources.

The background noise, unmatched antenna noise due to loss and the noise due to the matching network loss are respectively expressed by the mean square voltage sources,

$$V_{nb} = \sqrt{4N_0R_a} \tag{5}$$

$$V_{na} = \sqrt{4N_0R_{Al}} \tag{6}$$

$$V_{nm} = \sqrt{4N_0R_{Ml}} \tag{7}$$

where $N_0 = kT_0\Delta f$ is the thermal noise power at the room temperature T_0, k is Boltzmann's constant and Δf is the bandwidth. R_a is the radiation resistance of the antenna in the series circuit model shown in rightmost column of Fig.1(a)(b). R_{Al} represents the loss of the antenna and R_{Ml} represents the loss of the matching network. X_A represents the unmatched antenna reactance and X_{M1} and X_{M2} are the reactance of the matching network which is often split into two parts to serve both the purpose of resonating with the antenna reactance and transforming the antenna impedance to a standard interface impedance, say 50Ohm. This is also a good model for self-resonance ESAs where the impedance matching mechanisms are often built into the radiating elements (such as a meandered small dipole). The received signal power can be described by its mean square voltage,

$$V_s = \sqrt{4S_0R_a} \tag{8}$$

where S_0 is the maximum possible signal power the antenna can receive when antenna loss and matching network loss are absent. Note that Fig.1 assumes a series connection of these various noise sources and the signal source, which assumes that the radiated power, Ohmic loss of the antenna and Ohmic loss of the matching network are proportional to the square of a common current flowing on the antenna port. This is true for ESAs simply consisting of conductor wires such as dipoles and loops. The matching network is also simplified to a single reactive element. The antenna loss and matching network loss in these cases are Ohmic resistances of the wires and the matching elements. For other type of ESAs, such as those with dielectric material or more sophisticated matching networks, a combined series and parallel circuit model may be used instead. The resistances in the model will then be transformed to composite versions of the originally defined radiation resistance, Ohmic resistances and dielectric losses, yet a similar noise analysis can be conducted.

The signal to noise ratio of the incident wave is defined at the wave port, as the ratio between the power density of the electromagnetic waves from the transmitter arriving the input of the antenna comparing to that from the background thermal emission. This is given by,

$$SNR_i = \frac{V_s^2}{V_{nb}^2} = \frac{S_0}{N_0} \tag{9}$$

Assuming the detectors are noiseless, the signal to noise ratio at the output of the antenna is given by the mean square of the signal voltage versus the noise voltage at the input of the detector, all through a common voltage division,

$$SNR_o = \frac{d^2V_s^2}{d^2\left(V_{nb}^2 + V_{na}^2 + V_{nm}^2\right)} = \frac{R_a}{R_a + R_{Al} + R_{Ml}}\frac{S_0}{N_0} = \frac{\zeta S_0}{N_0} = \zeta SNR_i \tag{10}$$

where d is the voltage division ratio between X_{M2} and the rest of the impedances in the loop, i.e.

$$d = \left|\frac{jX_{M2}}{R_a + R_{Al} + R_{Ml} + jX_{M1} + jX_{M2}}\right| \tag{11}$$

ζ is the radiation efficiency of the antenna including the matching network loss, defined as,

$$\zeta = \frac{R_a}{R_a + R_{Al} + R_{Ml}} \tag{12}$$

Noise figure of the antenna can thus be obtained as the degradation of the SNR performance at the output of the antenna from that in the waves arriving at the antenna,

$$NF_A = \frac{SNR_i}{SNR_o} = \frac{1}{\zeta} = \frac{R_a + R_{Al} + R_{Ml}}{R_a} \tag{13}$$

It should be noted from (13) that the noise figure of the antenna is the inverse of the radiation efficiency not the total radiation efficiency that includes impedance match. Both the radiation efficiency and the noise figure of the antenna are not impacted by the input impedance of the noiseless detector as it will not alter the ratio of the signal voltage versus the noise voltage at the detector input. The reactance of the antenna does not impact the radiation efficiency and noise figure either. The radiation efficiency in (12) and noise figure expressed in (13) are both frequency dependent as both radiation resistance of ESAs and Ohmic resistances are weakly frequency dependent as given by (2). In general, assuming a constant Ohmic resistance R_{Al}, the radiation efficiencies of electrically small dipoles decrease according to the second order of the frequency and those of electrically small loops decrease as the fourth order of the frequency. Yet the behavior is generally broadband as it is not directly impacted by the resonant behavior of the antenna or the matching network.

From (12) and (13), it is evident that a lossless matching network changes neither the radiation efficiency nor the noise figure of an unmatched antenna while a practical matching network always adds loss and deteriorates the antenna's radiation efficiency and noise figure. A matching network may thus be unnecessary if a detector that is close to noiseless and with sufficient gain is used. This is in contrast to the traditional practices where it is assumed that the detector is noisy and with limited gain and a matching network is needed so that the received signal power can overcome the added noise by the detector and reach the latter stages of the receiver.

When the antenna structure or the matching element is of limited quality factors, one has the following definitions for antenna material quality factor and matching network quality factor,

$$Q_{am} = \frac{|X_A|}{R_{Al}}, \quad Q_{match} = \frac{|X_{M1} + X_{M2}|}{R_{Ml}} \tag{14}$$

Recall that the radiation quality factor of the antenna,

$$Q_{rad} \approx \frac{|X_A|}{R_a} \tag{15}$$

the antenna noise figure according to (13) thus becomes,

$$NF_A = 1 + \frac{Q_{rad}}{Q_{am}} + \frac{Q_{rad}}{Q_{match}} \tag{16}$$

It is evident that from (16) that a high radiation quality factor deteriorates the noise figure of an antenna when the quality factors of the antenna material and matching networks are not as high. However, as (13) indicates the noise figure of the antenna is weakly frequency dependent, the radiation quality factor is not fundamentally limiting the bandwidth of the receiver SNR like how it does in limiting the efficiency bandwidth product of a transmitter with the same antenna [12].

To represent the broadband behavior of antenna Ohmic loss, one could also define the antenna's cutoff frequency for electrically small dipole antennas and loop antennas separately as,

$$\begin{cases} \omega_{ac} = \dfrac{1}{C_a R_{Al}}, & Q_{am} = \dfrac{1}{\omega C_a R_{Al}} = \dfrac{\omega_{ac}}{\omega} \\ \quad (\textit{electrically small dipole}) & \\ \omega_{ac} = \dfrac{R_{Al}}{L_a}, & Q_{am} = \dfrac{\omega L_a}{R_{Al}} = \dfrac{\omega}{\omega_{ac}} \\ \quad (\textit{electrically small loop}) & \end{cases} \tag{17}$$

Ignore the matching network loss, the radiation efficiency and noise figure of the antenna can thus be written as,

$$\begin{cases} NF_A = \dfrac{1}{\zeta} = 1 + \dfrac{Q_{rad}}{Q_{am}} = 1 + \dfrac{\omega_{at}^3}{\omega^3}\dfrac{\omega}{\omega_{ac}} = 1 + \dfrac{\omega_{at}^3}{\omega^2 \omega_{ac}} \\ \quad (\textit{electrically small dipole}) \\ NF_A = \dfrac{1}{\zeta} = 1 + \dfrac{Q_{rad}}{Q_{am}} = 1 + \dfrac{\omega_{at}^3}{\omega^3}\dfrac{\omega_{ac}}{\omega} = 1 + \dfrac{\omega_{at}^3 \omega_{ac}}{\omega^4} \\ \quad (\textit{electrically small loop}) \end{cases} \tag{18}$$

The composite antenna quality factor excluding matching network loss is thus yielded as,

$$Q_A = \frac{|X_A|}{R_a + R_{Al}} = \frac{1}{\frac{1}{Q_{rad}} + \frac{1}{Q_{am}}} \tag{19}$$

B. SENSITIVITY DEFINED AS THE LOWEST DETECTABLE FIELD PER ROOT UNIT BANDWIDTH

For a lossless antenna, the thermal radiation received by the antenna is the only noise source and it sets the lowest detectable field per root unit bandwidth. Based on the equivalent circuit model in Fig.2, the open circuit noise mean square voltages are generated by the antenna radiation resistance at the environment temperature and they equal to the electric field of the noise multiplying the length of the dipole for electrically small dipoles or the electromotive force excited by the noise magnetic field for electrically small loops, which are expressed as,

$$V_{nb,dipole} = \sqrt{4N_0 R_{a,dipole}} = \sqrt{4kT_0 \Delta f R_{a,dipole}} = E_n \cdot l \tag{20}$$

$$V_{nb,loop} = \sqrt{4N_0 R_{a,loop}} = \sqrt{4kT_0 \Delta f R_{a,loop}} = \omega B_n S \tag{21}$$

where E_n and B_n are respectively the electric field at an electrically small dipole and the magnetic flux density at an electrically small loop generated by thermal radiation. l is the length of the dipole and S is the area enclosed by the loop and

R_a are radiation resistances for electrically small dipoles and loops respectively, given by the antenna theory [30],

$$R_{a,dipole} = 80\pi^2\left(\frac{l}{\lambda}\right)^2, R_{a,loop} = 320\pi^4\left(\frac{S}{\lambda^2}\right)^2 \quad (22)$$

Substituting (22) into (20) and (21) yields the electric field and the magnetic flux density per root unit bandwidth generated by the thermal noise incident on both ideal electrically small dipole and electrically small loops,

$$\frac{E_n}{\sqrt{\Delta f}} = \frac{\pi f}{c}\sqrt{320kT_0} \quad (23)$$

$$\frac{B_n}{\sqrt{\Delta f}} = \frac{\pi f}{c^2}\sqrt{320kT_0} \quad (24)$$

where c is the speed of light. Based on (23) and (24), the thermal noise field at the antenna for room temperature $T_0 = 290K$ at 10MHz are calculated to be 1.18×10^{-10}V/m and 3.95×10^{-19}T respectively for electrically small dipoles and electrically small loops. The sensitivity of a lossy antenna defined as the minimum detectable field per root hertz can now be obtained by multiplying (23) and (24) with the square root of the noise figure or divide them by the square root of its radiation efficiency, which are,

$$\frac{E}{\sqrt{\Delta f}} = \sqrt{NF_A}\cdot E_n = \frac{\pi f}{c}\sqrt{NF_A\cdot 320kT_0} = \frac{\pi f}{c}\sqrt{320kT_0/\zeta} \quad (25)$$

$$\frac{B}{\sqrt{\Delta f}} = \sqrt{NF_A}\cdot B_n = \frac{\pi f}{c^2}\sqrt{NF_A\cdot 320kT_0} = \frac{\pi f}{c^2}\sqrt{320kT_0/\zeta} \quad (26)$$

For example, a planar dipole made of copper with the maximum dimension of 24cm has a radiation efficiency of 2.7% at 10MHz and a planar loop made of 20um copper printed circuit board with the same maximum dimension has a radiation efficiency of 0.4% according to a full-wave simulator with the same setup as described in Section VII. This translates to an electric field sensitivity of 7.18×10^{-10}V/m and magnetic field sensitivity of 6.25×10^{-18}T. Taking the latter number, it means that a standard loop antenna made of copper can have a field sensitivity several orders better at 10MHz than a SQUID at DC. However, the radiation efficiency described by (12) drops off quickly for lower frequency according to the fourth order of the frequency and it is thus projected that the sensitivity for these technologies become comparable at around 1MHz.

IV. NOISE CONTRIBUTION FROM DETECTORS WITH INFINITE GAIN

The role of detectors is to amplify the received signal so that the SNR will no longer be affected by the noise added by the latter stage. Many forms of detectors have been applied to the detection of the electromagnetic field at different frequency bands, including various magnetometers (such as SQUID, Optical pumped magnetometers and RF Precession Modulation sensors) that are applied for detection of very low frequency (VLF) or ultra low frequency (ULF) magnetic fields. In HF/VHF bands, the most often seen type of detectors are low noise transistor amplifiers. The noise model of an ideal field effect transistor (FET) low noise amplifier (LNA) is illustrated in Fig.3 to represent the loss mechanisms specifically related to the gate resistance of the transistor. The same model could be applied to parametric amplifiers where the source of the noise in the detectors is the Ohmic resistance of the varactor diodes resulting limited quality factor. In general, all the detectors add loss thus thermal noise to the input signal and similar models can be established for all.

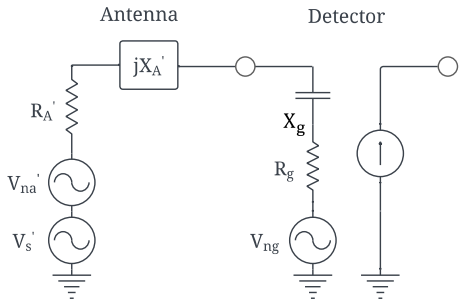

FIGURE 3. Noise model of a detector that is a FET amplifier.

One assumption often made in the literature is that the detector adds the same amount of noise as the thermal noise received by the antenna [29]. This is generally not true with the modern technology as it implies a 3dB minimum noise figure for a detector or a matched resistor inserted in front of a lossless detector. Even commercially off the shelf (COTS) LNAs can realize less than 0.5dB noise figure routinely at HF/VHF. This assumption of fixed amount of added noise also leads to an erroneous conclusion that the noise figure matching bandwidth of ESAs is fundamentally limited to the impedance matching bandwidth imposed by Harrington-Chu's limit [11], [12], [13] as it ignored the fact that the antenna impedance may significantly alter the amount of the noise added by the detector.

In Fig.3, the antenna impedance is represented by a general impedance parameter with its resistive component of R'_A and reactive component X'_A. It should be noted that these two impedance components could be strongly frequency dependent as they are transformed from the original impedances of the antenna in Fig.2 including matching networks. In the ideal transistor model shown Fig.3, it is assumed that the gain of the transistor is sufficiently high so that the noise added by the latter stage, including that generated by the drain to source channel resistance can be ignored and the drain/source to the gate coupling (such as those through Miller capacitance) is absent. The gate resistance R_g is thus the sole source of the noise added by the detector and it will be demonstrated that the contribution of the detector to the overall SNR is impacted by the matching between the gate and the antenna impedance. X_g is the gate capacitance and the voltage across

this capacitance is controlling the current source at the output and it is thus concluded the overall SNR of the detector output can be obtained by evaluating the signal voltage versus the noise voltage across this capacitor. In Fig.3, the root mean square (RMS) signal voltage, noise source voltage from the antenna and noise source voltage of the gate resistance are given respectively by,

$$V_s' = \sqrt{4\zeta S_0 R_A'} \tag{27}$$

$$V_{na}' = \sqrt{4N_0 R_A'} \tag{28}$$

$$V_{ng} = \sqrt{4N_0 R_g} \tag{29}$$

The RMS signal voltage and noise voltages across the gate capacitor are then given by voltage division, which are,

$$v_{c,s} = Q_g \frac{R_g}{R_A' + jX_A' + jX_g + R_g} \sqrt{4\zeta S_0 R_A'} \tag{30}$$

$$v_{c,na} = Q_g \frac{R_g}{R_A' + jX_A' + jX_g + R_g} \sqrt{4N_0 R_A'} \tag{31}$$

$$v_{c,ng} = Q_g \frac{R_g}{R_A' + jX_A' + jX_g + R_g} \sqrt{4N_0 R_g} \tag{32}$$

where Q_g is the quality factor of the gate defined by,

$$Q_g = \frac{|X_g|}{R_g} = \frac{1}{\omega C_g R_g} \tag{33}$$

For convenience of discussions later, a gate cutoff frequency ω_{gc} can be defined when Q_g defined in (33) reduces to one, which is,

$$\omega_{gc} = \frac{1}{R_g C_g}, \quad Q_g = \frac{\omega_{gc}}{\omega} \tag{34}$$

The signal to noise ratio at the output of the detector is thus yielded as the ratio between the mean square voltage of the signal versus that of the noise, i.e.,

$$SNR_t = \frac{v_{c,s}^2}{v_{c,ng}^2 + v_{c,n0}^2} = \frac{\zeta S_0}{N_0} \frac{R_A'}{R_A' + R_g} = \frac{\zeta S_0}{N_0} \left(\frac{1}{1 + \frac{R_g}{R_A'}} \right) \tag{35}$$

The noise figure of the receiver with ESA is thus obtained as,

$$NF = \frac{SNR_i}{SNR_t} = \frac{1}{\zeta} \left(1 + \frac{R_g}{R_A'} \right) \tag{36}$$

From (35) and (36), it is evident that to maximize the SNR and minimize the noise figure one should maximize R_A' and minimize R_g, until the detector gain falls off to a level that the latter stage added noise becomes comparable. This is what is behind the conventional noise matching principles in low noise amplifiers [32].

On the other hand, it is not difficult to derive the detector output SNR as a function of the reflection coefficient looking out from the gate resistance of the detector, which is,

$$SNR_t = \frac{\left(1 - |\Gamma|^2\right) S_0}{\left(1 - |\Gamma|^2\right) N_0 + |1 - \Gamma|^2 N_0} \tag{37}$$

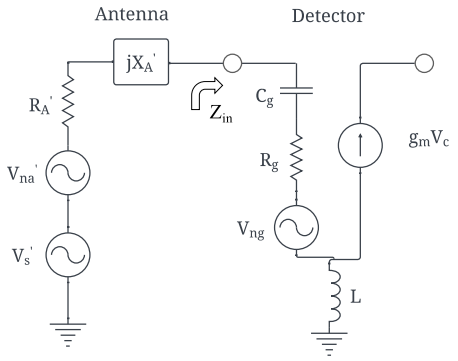

FIGURE 4. Noise model of a FET detector with a source degenerating inductor.

where the reflection coefficient is defined as,

$$\Gamma = \frac{R_A' + jX_A' + jX_g - R_g}{R_A' + jX_A' + jX_g + R_g} \tag{38}$$

It is evident from (37) that mismatch reduces both the input signal power and the injected background noise power by the same ratio, while it also affects the noise power added to the system by the detector. Under the conjugate matching condition $\Gamma = 0$, the gain of the detector is maximized, (37) gives the SNR as,

$$SNR_t = \frac{\zeta}{2} \frac{S_0}{N_0} \tag{39}$$

The SNR drops by 3dB as the result of conjugate match. In general, under a high impedance match where Γ is real and positive, it is yielded,

$$SNR_t = \zeta \frac{\Gamma + 1}{2} \frac{S_0}{N_0} \tag{40}$$

The SNR is maximized by setting $\Gamma \approx 1$. Assuming that the gain of the detector is still sufficient under this severely mismatched condition, the yielded SNR is almost as good as that of the SNR of the antenna output.

One confusion that exists among many is that the input impedances of many COTS amplifiers behave like 50Ohm which makes them appear to be conjugately matched to 50Ohm sources yet they offer a noise figure much less than 3dB. This seems to contradict with the conclusion in (39). This is because the reflection coefficient looking into the input of the amplifier could significantly differ from the reflection coefficient looking out from the gate resistance of the amplifier, particularly when a source degenerating inductor is used in the detector. Such a detector is shown in Fig.4, the source of the FET is connecting to the ground through an inductor L.

A simple circuit analysis reveals that the input voltage and current to the detector is related by the following equation,

$$\begin{aligned} V_{in} &= I_{in} \left(\frac{1}{j\omega C_g} + R_g \right) + \mathrm{j}\omega L \cdot \frac{g_m I_{in}}{j\omega C_g} \\ &= I_{in} \left(\frac{1}{j\omega C_g} + R_g + \frac{g_m L}{C_g} \right) \end{aligned} \tag{41}$$

where g_m is the transconductance of the transistor. The input impedance is thus given by,

$$Z_{in} = \frac{1}{j\omega C_g} + R_g + \frac{g_m L}{C_g} \tag{42}$$

It is observed from the third term in the righthand side of (42) that the source degenerating inductor increases the resistive component of the input impedance by a factor g_m and it now can be easily matched to a 50Ohm standard impedance. However, the reflection coefficient as defined by (38) can remain high for noise match and the signal and RMS noise voltages across the gate capacitor become,

$$v_{c,s} = Q_g \frac{R_g}{R'_A + jX'_A + Z_{in}} \sqrt{4\zeta S_0 R'_A} \tag{43}$$

$$v_{c,na} = Q_g \frac{R_g}{R'_A + jX'_A + Z_{in}} \sqrt{4N_0 R'_A} \tag{44}$$

$$v_{c,ng} = Q_g \frac{R_g}{R'_A + jX'_A + Z_{in}} \sqrt{4N_0 R_g} \tag{45}$$

The voltage division relations in (43)-(45) are modified with the same constant. Therefore, even though Z_{in} is now different from the non-degenerating case, the signal to noise ratio remains the same as what are described in (35) and (37) and the noise figure of the receiver is not impacted by the source degenerating inductor.

V. NOISE MATCHING OPTIONS BETWEEN AN ESA AND A DETECTOR

With the above analyses, it is now clear that one must jointly design the antenna with the detector to obtain the best SNR and the maximum bandwidth of noise matching. Equalizing both antenna circuit models from Fig.2 and Fig.3 as shown in Fig.5 results in,

$$R'_A + jX'_A = \frac{jX_{M2}\left(R_a + R_{Al} + R_{Ml} + jX_A + jX_{M1}\right)}{R_a + R_{Al} + R_{Ml} + jX_A + jX_{M1} + jX_{M2}} \tag{46}$$

In particular, the real part of the antenna impedance takes the form,

$$R'_A = \frac{X_{M2}^2\left(R_a + R_{Al} + R_{Ml}\right)}{\left|R_a + R_{Al} + R_{Ml} + jX_A + jX_{M1} + jX_{M2}\right|^2} \tag{47}$$

Several noise matching options are discussed as below.

A. RESONANCE MATCH OF THE ANTENNA TO 50OHM

One often seen matching option is to create a resonance at a center frequency by selecting $X_A + X_{M1} + X_{M2} = 0$ at this angular frequency ω_r, and the real part of the impedance at resonance thus becomes,

$$R'_A(\omega_r) = \frac{X_{M2}^2}{R_a + R_{Al} + R_{Ml}} \tag{48}$$

By selecting the appropriate value of X_{M2}, R'_A can be scaled up and down until a 50Ohm impedance is created. A low noise figure at the resonance could be achieved as the gate resistance R_g of a typical transistor is usually much lower than 50Ohm or it could be transformed to a value much lower than 50Ohm through an amplifier matching network. This option is a good representation of many existing designs of self-resonance ESAs that often have a pre-matched output impedance of 50Ohm. The noise figure of the receiver including the ESA in dB scale is obtained from (36) as,

$$\begin{aligned} NF\ [dB] &\approx 10log10\left(\frac{1}{\zeta}\right) + 10\log_{10}\left(1 + \frac{R_g}{R'_A}\right) \\ &= NF_A\ [dB] + NF_d\ [dB] \end{aligned} \tag{49}$$

where NF_d is the noise figure contributed by the detector and at resonance it is,

$$\begin{aligned} NF_d\left(\omega_r\right) &= 10\log_{10}\left[1 + \frac{R_g}{R'_A\left(\omega_r\right)}\right] \\ &= 10\log_{10}\left(1 + \frac{R_g}{50}\right) \end{aligned} \tag{50}$$

This noise figure degrades to 3dB when

$$R'_A\left(\omega_r + \Delta\omega\right) = R_g \tag{51}$$

On the other hand, in the proximity of the resonance, the antenna impedance can be approximated by [32],

$$Z'_A\left(\omega_r + \Delta\omega\right) \approx \frac{R'_A\left(\omega_r\right)}{\left(1 + 2jQ_A\frac{\Delta\omega}{\omega_r}\right)} \tag{52}$$

where Q_A is the composite antenna quality factor given by,

$$Q_A = \frac{|X_A|}{R_a + R_{Al} + R_{Ml}} \tag{53}$$

The antenna resistance is thus given by,

$$R'_A\left(\omega_r + \Delta\omega\right) \approx \frac{R'_A\left(\omega_r\right)}{1 + \left(2Q_A\frac{\Delta\omega}{\omega_r}\right)^2} \tag{54}$$

Joining (51) and (54) derives the 3dB noise figure degradation bandwidth by,

$$\frac{2\Delta\omega}{\omega_r} \approx \frac{1}{Q_A}\sqrt{\frac{R'_A\left(\omega_r\right)}{R_g} - 1} \approx \frac{1}{Q_A}\sqrt{\frac{50}{R_g}} \tag{55}$$

It is thus evident from (55) that the 3dB noise matching bandwidth is greater than the 3dB impedance matching bandwidth of the antenna (the one defined by the inverse of the antenna quality factor) by a factor of $\sqrt{50/R_g}$ even with such a standard matching technique. The noise matching bandwidth equals to the conjugate impedance matching bandwidth only when the gate resistance of the detector is equal to the antenna resistance which is rarely the case with the modern semiconductor technology.

B. RESONANCE MATCH OF THE ANTENNA TO THE HIGHEST OUTPUT IMPEDANCE

In this option, it is selected that $X_{M1} = 0$ and $X_{M2} = -X_A$ to maximize the transformed antenna impedance. The antenna resistance in (48) becomes,

$$R'_A\left(\omega_r\right) = \frac{X_A^2}{R_a + R_{Al} + R_{Ml}} = Q_A^2(R_a + R_{Al} + R_{Ml}) \tag{56}$$

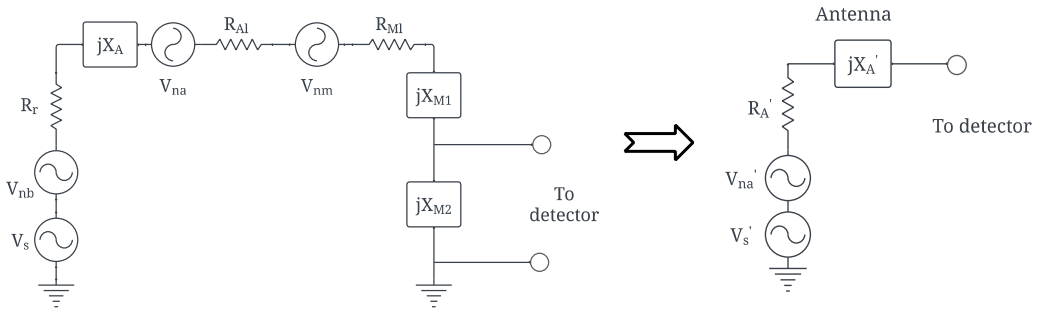

FIGURE 5. Noise matching options between the antenna and the detector.

This is the highest impedance that can be achieved for the antenna output without incurring an additional matching network. As indicated by (36), the noise figure is minimized when the ratio of R'_A/R_g is maximized as long as a sufficient detector gain can be retained. The state-of-the-art transistors have cutoff frequencies of several hundreds of GHz, which can help to achieve a positive gain at the HF/VHF band even under this severely mismatched case. Therefore, this option typically gives better signal to noise performance comparing to option (a) without requiring a large transistor periphery or an additional transistor matching network, which is,

$$NF_d\,(\omega_r)\,[dB] = 10\log_{10}\left[1+\frac{R_g}{R'_A\,(\omega_r)}\right] = 10\log_{10}\left[1+\frac{R_g}{Q_A^2\,(R_a+R_{Al}+R_{Ml})}\right] \tag{57}$$

It is evident from (57) that a smaller noise figure at the center frequency can be achieved comparing to (50) as the transformed antenna impedance is often much higher than 50Ohm. The 3dB bandwidth of the noise match follows the same relation as indicated in (55), which is

$$\frac{2\Delta\omega}{\omega_r} \approx \frac{1}{Q_A}\sqrt{\frac{R'_A\,(\omega_r)}{R_g}} = \frac{1}{Q_A}\sqrt{\frac{Q_A^2\,(R_a+R_{Al}+R_{Ml})}{R_g}} = \sqrt{\frac{R_A}{R_g}} \tag{58}$$

The 3dB noise figure bandwidth at this case could also be much wider than option (a) yet the power consumption of the transistor is expected to be minimum. Unfortunately, the noise figure bandwidth predicted by (58) is often not achievable in practice due to the limited gain of a practical detector under this severe mismatch condition. The output noise (drain current) noise soon becomes a limiting factor as it will be shown in the next section.

C. DIRECT MATCH OF THE ANTENNA TO THE DETECTOR

An alternative way of matching the antenna to the detector is to connect the antenna directly to a detector without going through a matching network, which is called active direct matching. This is the case when one sets $X_{M1} = 0$ and $X_{M2} = \infty$ in Fig.5. The antenna resistance then becomes,

$$R'_A = R_A = R_a + R_{Al} \tag{59}$$

In contrast to the transformed, narrow band antenna resistance expression in (48) or (56), the antenna resistance obtained in (59) is broadband as no resonance match or associated impedance transformation is applied. Its frequency dependence primarily rises from the dispersion of the radiation resistance when a series equivalent circuit model is derived for the ESA as shown by (2). The matching network resistance R_{Ml} no longer exists in the antenna resistance due to the absence of the matching network. For this reason, the overall antenna noise figure often improves according to (36) over the case when a resonance match is used. With active direct matching, the noise figure of the detector could remain low over a broad bandwidth as long as R_g could be made much smaller than R'_A. As the radiation resistance of the ESA is hard to modify in a broadband sense, the easiest way to yield a good noise figure is to scale the periphery of the transistor so that its gate resistance can be much lower than the antenna's radiation resistance. This option is expected to provide the broadest noise matching bandwidth.

To gain a balance between the noise matching bandwidth and the power consumption of the amplifiers, one could choose $X_{M1} = 0$ and $1/X_{M2} + 1/X_g = -1/X_A$. This means, the resonance is realized by canceling the antenna's reactance with a combination of a passive reactance and the reactance of the detector. Selecting the ratio between these two admittances can lead to either option (c) ($1/X_{M2} = 0$) or option (b) ($1/X_g \approx 0$) or a compromised matching characteristics between options (b) and (c). This applies to the case of an electrically small loop antenna which is to be matched either with a passive capacitor or the capacitance of a detector or a combination of both.

From the discussions above, it is concluded that the conventional resonance noise match can yield a high R'_A which can easily accommodate transistors with a small periphery and a high R_g. This means transistors with low power consumption can be used yet the noise figure can remain low. The SNR bandwidth, however, is often limited. It has been observed when electrical dimensions of antennas are much

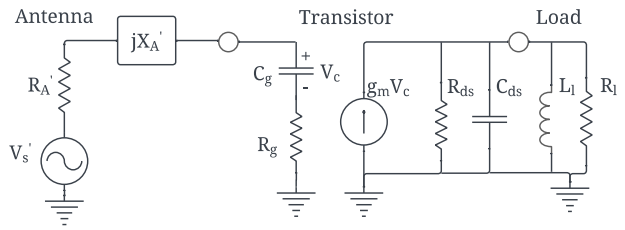

FIGURE 6. Noise matching of electrically small antennas.

smaller than ka = 1/4, the matching circuit loss increases significantly in conventional resonant noise matching which will dominate the noise figure if used. In this case, active direct matching offers better noise figure as the matching network and associated loss is absent. To yield a good noise figure with active direct matching, devices with low R_g are required which means transistors with large periphery are required which would incur greater power consumption yet the bandwidth is generally broader. For electrically small loops, the matching circuits are typically high-Q capacitors, therefore the hybrid matching could be explored for best SNR and bandwidth as well as the power consumption trade-off. For electrically small dipoles, the required matching circuits are inductors which are often with low-Q. Therefore, active direct matching is expected to offer superior system noise figure comparing to the other options as no inductor is needed.

VI. GAIN AND NOISE FIGURE OF ESA RECEIVER WITH DETECTORS THAT HAVE FINITE GAIN

Now we consider several matching options including both option (b) and (c) in section V for electrically small antennas when transistors with finite gain are used. Fig.6 shows the example of such matching with a FET. The transistor is now assumed to have a finite transconductance g_m and a drain to source resistance R_{ds} and capacitance C_{ds}. The output of the transistor is conjugately matched to a load with a load resistance of R_l. It should be noted that the transistor model shown in Fig.6 is still simplified from what is being used for practical designs for simplicity of discussions, as it assumes a uni-directional transfer characteristics and absence of Miller capacitance.

The gate noise is similarly derived as it was done in Section III, which includes two RMS noise voltages from the antenna and from the gate respectively,

$$\begin{aligned} V_{c,na} &= \frac{1}{\omega C_g}\frac{V_{na}}{\left|R'_A+R_g+jX'_A+jX_g\right|} \\ &= \frac{1}{\omega C_g}\frac{\sqrt{4N_0R'_A}}{\left|R'_A+R_g+jX'_A+jX_g\right|} \end{aligned} \tag{60}$$

$$\begin{aligned} V_{c,ng} &= \frac{1}{\omega C_g}\frac{V_{ng}}{\left|R'_A+R_g+jX'_A+jX_g\right|} \\ &= \frac{1}{\omega C_g}\frac{\sqrt{4N_0R_g}}{\left|R'_A+R_g+jX'_A+jX_g\right|} \end{aligned} \tag{61}$$

where R'_A is the transformed resistance of the unmatched antenna resistance and the Ohmic resistance as given by (46), X'_A is the transformed reactance of the antenna, $X_g = 1/\omega C_g$ is the reactance of the gate. The total noise voltage across the gate capacitance is the RMS summation of the two which yields,

$$V_{cn} = \sqrt{V_{c,na}^2+V_{c,ng}^2} = \frac{1}{\omega C_g}\frac{\sqrt{4N_0(R'_A+R_g)}}{\left|R'_A+R_g+jX'_A+jX_g\right|} \tag{62}$$

The total noise power at the output of the amplifier is the amplified version of the gate noise plus the noise power generated by the channel resistance. The open circuit noise voltage at the output of the transistor is thus given by,

$$\begin{aligned} V_{dn}^2 &= (g_mV_{cn}R_{ds})^2+\frac{4N_0}{R_{ch}}R_{ds}^2 \\ &= 4N_0R_{ds}^2\left[\left(\frac{g_m}{\omega C_g}\right)^2\frac{R'_A+R_g}{\left|R'_A+R_g+jX'_A+jX_g\right|^2}+\frac{1}{R_{ch}}\right] \end{aligned} \tag{63}$$

where R_{ch} is the channel resistance of the transistor. On the other hand, the RMS signal voltage across the gate capacitance of the transistor is given by,

$$\begin{aligned} V_{cs} &= \frac{1}{\omega C_g}\frac{V'_s}{\left|R'_A+R_g+jX'_A+jX_g\right|} \\ &= \frac{1}{\omega C_g}\frac{\sqrt{4\zeta S_0R'_A}}{\left|R'_A+R_g+jX'_A+jX_g\right|} \end{aligned} \tag{64}$$

At the output of the transistor, the open circuit signal voltage at the drain is yielded as,

$$\begin{aligned} V_{ds}^2 &= (g_mV_{cs}R_{ds})^2 \\ &= 4\zeta S_0\left(\frac{g_m}{\omega C_g}\right)^2\frac{R'_AR_{ds}^2}{\left|R'_A+R_g+jX'_A+jX_g\right|^2} \end{aligned} \tag{65}$$

Under the conjugate output match condition ($R_l = R_{ds}, \omega L_l = \frac{1}{\omega C_{ds}}$), the transducer gain of the receiver defined from the wave port to the output of the transistor amplifier becomes,

$$G_T = \frac{1}{4}\frac{V_{ds}^2}{R_l}\frac{1}{S_0} = \left(\frac{g_m}{\omega C_g}\right)^2\frac{\zeta R'_AR_{ds}}{\left|R'_A+R_g+jX'_A+jX_g\right|^2} \tag{66}$$

The noise figure of the receiver defined from the wave port is thus obtained as,

$$\begin{aligned} NF &= \frac{SNR_i}{SNR_t} = \frac{S_0}{N_0}\frac{V_{dn}^2}{V_{ds}^2} \\ &= \frac{1}{\zeta}\left[\frac{R'_A+R_g}{R'_A}+\left(\frac{\omega C_{gs}}{g_m}\right)^2\frac{\left|R'_A+R_g+jX'_A+jX_g\right|^2}{R'_AR_{ch}}\right] \end{aligned} \tag{67}$$

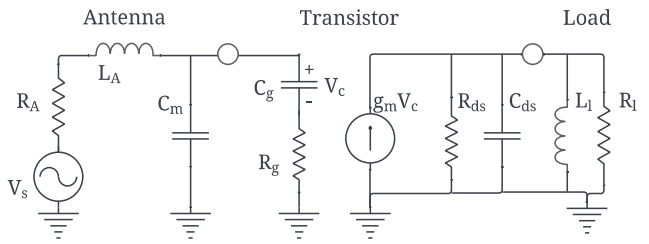

FIGURE 7. Noise matching of an electrically small loop antenna to a transistor.

Substituting (66) into (67) yields,

$$NF = \frac{1}{\zeta}\left(1 + \frac{R_g}{R'_A} + \frac{\zeta}{G_T}\frac{R_{ds}}{R_{ch}}\right) \tag{68}$$

Note that (68) reduces to (36) when the transducer gain tends to infinity.

Next we will discuss the specific noise matching options for electrically loop antennas and electrically small dipole antennas separately.

A. NOISE MATCHING OF AN ELECTRICALLY SMALL LOOP

When an electrically small loop antenna is being matched to a transistor, the equivalent circuit shown in Fig.7 can be used. The receiving antenna has a source resistance of R_A which is a summation of the antenna's radiation resistance and Ohmic resistance, given by,

$$R_A = R_a + R_{Al} \tag{69}$$

The inductance of the loop L_A is matched with a combination of an external capacitor of value C_m and the gate capacitance C_g. Ignore the resistance of the gate, the total capacitance looking out from the antenna is thus given by,

$$C_t \approx C_m + C_g = \beta C_g \tag{70}$$

where β is the capacitance ratio between the total capacitance and the gate capacitance which is a design parameter. A large β leads to the high impedance resonance matching, i.e. option (b) in Section IV and a smaller β or $\beta = 1$ gives active direct matching, i.e. option (c) in Section IV.

The antenna inductance resonates with the total capacitance at an angular frequency ω_r. The signal voltage across the gate capacitance is approximately equal to that across C_m, which is,

$$\begin{aligned} V_{cs} &= \frac{1}{\omega C_t}\frac{V_s}{\left|R_A + j\omega L_A + \frac{1}{j\omega C_T}\right|} \\ &= \frac{1}{\omega C_t}\frac{\sqrt{4\zeta S_0 R_A}}{\left|R_A + j\omega L_A + \frac{1}{j\omega C_T}\right|} \end{aligned} \tag{71}$$

At the output of the transistor, the open circuit signal voltage at the drain is yielded as,

$$\begin{aligned} V_{ds}^2 &= (g_m V_{cs} R_{ds})^2 \\ &= 4\zeta S_0 \left(\frac{g_m}{\omega C_t}\right)^2 \frac{R_A R_{ds}^2}{\left|R_A + j\omega L_A + \frac{1}{j\omega C_T}\right|^2} \end{aligned} \tag{72}$$

Under the conjugate output match condition, e.g., $R_l = R_{ds}$, the transducer gain of the receiver defined from the wave port to the output of the transistor amplifier becomes,

$$G_T = \frac{1}{4}\frac{V_{ds}^2}{R_l}\frac{1}{S_0} = \zeta\left(\frac{g_m}{\omega C_t}\right)^2 \frac{R_A R_{ds}}{\left|R_A + j\omega L_A + \frac{1}{j\omega C_T}\right|^2} \tag{73}$$

The noise figure is thus derived by substituting (73) into (68).

When $\beta \gg 1$ *or* $C_g < C_m$, the impact of transistor gate capacitance loading on resonant frequency can be ignored. Therefore, at this resonance frequency, the transformed antenna resistance is given by (56) which is,

$$R'_A(\omega_r) = Q_A^2 R_A \tag{74}$$

The transducer gain at the same condition is derived to be,

$$G_T(\omega_r) = \zeta\left(\frac{g_m}{\omega C_t}\right)^2 \frac{R_{ds}}{R_A} \tag{75}$$

The noise figure at the resonance is thus derived to be,

$$NF(\omega_r) = \frac{1}{\zeta}\left[1 + \frac{1}{Q_A^2}\frac{R_g}{R_A} + \left(\frac{\omega C_t}{g_m}\right)^2 \frac{R_A}{R_{ch}}\right] \tag{76}$$

Considering ω_T is the transition frequency of a transistor is given by,

$$\omega_T = \frac{g_m}{C_g} \tag{77}$$

The transducer gain from (75) thus becomes,

$$G_T(\omega_r) = \frac{\zeta}{Q_A}\frac{\omega_T}{\omega}\frac{g_m R_{ds}}{\beta} \tag{78}$$

Note that the transducer gain decreases with the increase of β. It is also known from the device theory that, the channel resistance of a FET is related to its transconductance by,

$$R_{ch} = \frac{1}{\gamma g_m} \tag{79}$$

where γ is a constant derived numerically or from measurements [33]. Substituting (79) into (76) becomes,

$$NF(\omega_r) = \frac{1}{\zeta}\left[1 + \frac{\beta}{Q_A Q_g} + \gamma\frac{\beta}{Q_A}\frac{\omega_r}{\omega_T}\right] \tag{80}$$

which indicates that a smaller capacitance coefficient β leads a better noise figure at the resonant frequency.

The transducer gain off the resonance can be characterized from (73) by [32],

$$\begin{aligned} G_T(\omega_r + \Delta\omega) &\approx \zeta\left(\frac{g_m}{\omega C_t}\right)^2 \frac{R_A R_{ds}}{\left|R_A\left(1 + 2jQ_A\frac{\Delta\omega}{\omega_r}\right)\right|^2} \\ &= \zeta\left(\frac{g_m}{\omega C_t}\right)^2 \frac{R_{ds}}{R_A}\frac{1}{1 + \left(2Q_A\frac{\Delta\omega}{\omega_r}\right)^2} \end{aligned} \tag{81}$$

Recall (54), a similar characterization applies,

$$R'_A(\omega_r+\Delta\omega)\approx\frac{R'_A(\omega_r)}{1+\left(2Q_A\frac{\Delta\omega}{\omega_r}\right)^2}=\frac{Q_A^2R_A}{1+\left(2Q_A\frac{\Delta\omega}{\omega_r}\right)^2} \tag{82}$$

Substituting (81) and (82) in (68) yields the noise figure off the resonance,

$$NF(\omega_r+\Delta\omega)\approx\frac{1}{\zeta}\left\{1+\left[\frac{1}{Q_A^2}\frac{R_g}{R_A}+\left(\frac{\omega C_t}{g_m}\right)^2\frac{R_A}{R_{ch}}\right]\left[1+\left(2Q_A\frac{\Delta\omega}{\omega_r}\right)^2\right]\right\} \tag{83}$$

Or alternatively, it can be expressed as,

$$NF(\omega_r+\Delta\omega)\approx\frac{1}{\zeta}\left\{1+\frac{\beta\omega}{Q_A}\left[\frac{1}{\omega_{gc}}+\frac{\gamma}{\omega_T}\right]\left[1+\left(2Q_A\frac{\Delta\omega}{\omega_r}\right)^2\right]\right\} \tag{84}$$

Off the resonance, the 3dB detector noise figure bandwidth is derived by setting the second term of (84) to 1, i.e.,

$$\frac{\beta\omega}{Q_A}\left[\frac{1}{\omega_{gc}}+\frac{\gamma}{\omega_T}\right]\left[1+\left(2Q_A\frac{\Delta\omega}{\omega_r}\right)^2\right]=1 \tag{85}$$

which yields the 3dB noise match fractional bandwidth as,

$$\frac{2\Delta\omega}{\omega_r}\approx\frac{\frac{1}{Q_A}}{\sqrt{\frac{\beta\omega}{Q_A}\left[\frac{1}{\omega_{gc}}+\frac{\gamma}{\omega_T}\right]}}=1/\sqrt{\beta\omega Q_A\left[\frac{1}{\omega_{gc}}+\frac{\gamma}{\omega_T}\right]} \tag{86}$$

For high efficiency antennas, $Q_A\approx Q_a=\omega_{at}^3/\omega^3$ where ω_{at} is the antenna transition frequency defined by (4). One yields the fractional bandwidth as,

$$\frac{2\Delta\omega}{\omega_r}\approx\sqrt{\frac{\omega^2}{\beta\omega_{at}^3}\left(\frac{\omega_T\omega_{gc}}{\omega_T+\gamma\omega_{gc}}\right)} \tag{87}$$

It is thus concluded that a smaller β also helps to achieve a wider 3dB noise bandwidth at the price of a larger transistor periphery and greater power consumption.

Now in the active direct matching case, $\beta=1$, the electrically small loop antenna with an inductance L_a is resonating with the capacitance of the transistor with a periphery so that $\omega_r L_a=\frac{1}{\omega_r C_g}$ at an angular frequency ω_r. Note that $R'_A=R_A$, the transducer gain from (68) at the resonance becomes,

$$G_T(\omega_r)=\zeta\left(\frac{g_m}{\omega C_g}\right)^2\frac{R_AR_{ds}}{(R_A+R_g)^2} \tag{88}$$

A high transducer gain can be achieved at the resonance, which will result in a noise figure very close to what is given in (36). Recall Q_A and Q_g are quality factors of the antenna and the gate of the transistor respectively given by (53) and (33), the antenna quality factor of electrically small loop can also be expressed as a function to the gate capacitance by,

$$Q_A=\frac{\omega L_a}{R_A}=\left(\frac{\omega}{\omega_r}\right)^2\frac{1}{\omega R_A C_g} \tag{89}$$

The noise figure around the resonance is dominated by the gate noise. With (89) substituted into (68), it becomes,

$$NF(\omega\approx\omega_r)\approx\frac{1}{\zeta}\left(1+\frac{R_g}{R_A}\right)=\frac{1}{\zeta}\left[1+\left(\frac{\omega_r}{\omega}\right)^2\frac{Q_A}{Q_g}\right]=\frac{1}{\zeta}\left[1+\frac{\omega_r^2\omega_{at}^3}{\omega_{gc}\omega^4}\right] \tag{90}$$

and ω_{gc} is the cutoff frequency of the gate given by (34). From (84), it is concluded that the noise figure at a frequency higher than the resonant frequency is lower. It is thus preferred to use a resonant frequency lower than the desired operating frequency. One convenient choice is to set the resonant frequency as the 3dB noise figure lower bound of the operating frequency as the noise figure would rise up sharply below that frequency according to the 4$^{\text{th}}$ order of the frequency as evidenced in (90). The gate noise contribution, i.e., the second term in (90) becomes 1 when $\omega=\omega_r$, e.g.,

$$\left(\frac{\omega_r}{\omega}\right)^2\frac{Q_A}{Q_g}=\frac{\omega_{at}^3}{\omega_{gc}\omega^2}=1 \tag{91}$$

This lower bound is thus found to be,

$$\omega_L=\omega_r=\omega_{at}\sqrt{\frac{\omega_{at}}{\omega_{gc}}} \tag{92}$$

The trend described by (90), i.e., the reduction of noise figure with the increase of the frequency continues until the transducer gain falls off, which is often at a frequency much higher than the resonance frequency given by,

$$G_T(\omega\gg\omega_r)\approx\zeta\left(\frac{g_m}{\omega C_g}\right)^2\frac{R_AR_{ds}}{(\omega L_A)^2}=\zeta\frac{\omega_r^2}{\omega^3}\frac{g_m\omega_T}{Q_A}R_{ds}=\zeta\frac{\omega_r^2\omega_T}{\omega_{at}^3}g_mR_{ds} \tag{93}$$

which is a frequency independent constant once the resonance frequency is set. Note that the gate noise expression by (90) is broadband, substituting the transducer gain expression (93) into (68) and combining the gate noise expression (90) yields the total noise figure as,

$$NF(\omega\gg\omega_r)\approx\frac{1}{\zeta}\left[1+\frac{\omega_r^2\omega_{at}^3}{\omega_{gc}\omega^4}+\gamma\frac{\omega_{at}^3}{\omega_r^2\omega_T}\right] \tag{94}$$

Assuming the gate noise, i.e., the second term in (94) can be minimized by choosing a resonant frequency sufficiently low, the upper bound of the 3dB noise figure bandwidth excluding antenna efficiency loss can thus be estimated when the drain noise contribution, i.e. the third term in (94) becomes unity,

$$\gamma\frac{\omega_{at}^3}{\omega_r^2\omega_T}=1 \tag{95}$$

Note that lefthand side of (95) is determined by the technology and the design and not by the operating frequency. This implies a flat noise figure when the operating frequency is much higher than the resonant frequency and thus the upper bound of 3dB noise figure operation may not exist. However, the noise figure in the higher end of the frequency is impacted by the selection of the resonant frequency. In contrast to some traditional assertions that the 3dB noise bandwidth is determined by the impedance matching bandwidth, e.g., the inverse of the antenna quality factor, (95) shows the low noise bandwidth of a receiver with an electrically small loop antenna is unlimited in its higher end and in the lower end it is determined by the ratio between the antenna transition frequency versus the gate cutoff frequency in the form of (90). Circuit simulation results will be presented in the next section to show that a very wide low noise bandwidth can be achieved at VHF with state of art transistors. However, it should also be noted that setting a low resonant frequency at the gate may require transistors with exceptionally large periphery and incur great power consumption.

B. ACTIVE DIRECT MATCHING OF ELECTRICALLY SMALL DIPOLES

An electrically small dipole with capacitance of C_a can be resonantly matched with a lumped inductor yet the limited Q of lumped inductors at HF/VHF (<60@100MHz) means a great amount of resistive noise will be added at the input. Alternatively, it can be directly matched to a transistor with a gate capacitance of C_g. Due to the fact both the antenna and the gate are being high-Q, the transducer gain from (66) now becomes,

$$\begin{aligned} G_T &= \zeta \left(\frac{g_m}{\omega C_g}\right)^2 \frac{R_A R_{ds}}{\left(X_A + X_g\right)^2} \\ &= \zeta \left(\frac{g_m}{C_g}\right)^2 \left(\frac{C_a C_g}{C_g + C_a}\right)^2 R_A R_{ds} \end{aligned} \tag{96}$$

Substituting the definitions of the transition frequency and antenna quality factor into (66) yields,

$$G_T = \zeta \frac{C_a C_g}{\left(C_g + C_a\right)^2} \frac{\omega_T}{\omega} \frac{1}{Q_A} g_m R_{ds} \tag{97}$$

Note that transition frequency, antenna quality factor and $g_m R_{ds}$ are all constants for a given technology and a given antenna design, one may select,

$$C_a = \beta C_g \tag{98}$$

The transducer gain then becomes,

$$G_T = \frac{\zeta \beta}{(\beta+1)^2} \frac{\omega_T}{\omega} \frac{1}{Q_A} g_m R_{ds} \tag{99}$$

Substituting (99) into (68) yields the noise figure as,

$$\begin{aligned} NF &= \frac{1}{\zeta}\left(1 + \frac{R_g}{R_A} + \frac{(\beta+1)^2}{\beta} \frac{1}{g_m^2} \frac{1}{R_A R_{ch}}\right) \\ &= \frac{1}{\zeta}\left(1 + \beta \frac{Q_A}{Q_g} + \frac{(\beta+1)^2}{\beta} \frac{\gamma Q_A \omega}{\omega_T}\right) \\ &= \frac{1}{\zeta}\left[1 + \frac{\omega_{at}^3}{\omega^2}\left(\frac{\beta}{\omega_{\text{gc}}} + \frac{(\beta+1)^2}{\beta} \frac{\gamma}{\omega_T}\right)\right] \end{aligned} \tag{100}$$

To maximize the transducer gain, the gate capacitance of the transistor should then be set to an optimum matching condition,

$$C_a = C_g \quad or \ \beta = 1 \tag{101}$$

The resulted maximum gain is,

$$G_T = \frac{\zeta}{4} g_m^2 R_A R_{ds} = \frac{\zeta}{4} \frac{\omega_T}{\omega} \frac{1}{Q_A} g_m R_{ds} \tag{102}$$

The noise figure at this condition is thus given by,

$$\begin{aligned} NF &= \frac{1}{\zeta}\left(1 + \frac{Q_A}{Q_g} + \frac{4\gamma Q_A \omega}{\omega_T}\right) \\ &= \frac{1}{\zeta}\left[1 + \frac{\omega_{at}^3}{\omega^2}\left(\frac{1}{\omega_{\text{gc}}} + \frac{4\gamma}{\omega_T}\right)\right] \end{aligned} \tag{103}$$

The lower bound of the 3dB noise figure operating frequency is derived by assuming the summation of the second and the third term in (103) equals to 1, which gives the condition of,

$$\frac{Q_A}{Q_g} + \frac{4\gamma Q_A \omega}{\omega_T} = \frac{\omega_{at}^3}{\omega^2}\left(\frac{1}{\omega_{\text{gc}}} + \frac{4\gamma}{\omega_T}\right) = 1 \tag{104}$$

The frequency lower bound is thus given by,

$$\omega_L = \omega_{at}^{1.5} \sqrt{\frac{1}{\omega_{gc}} + \frac{4\gamma}{\omega_T}} \tag{105}$$

The upper bound frequency does not exist either as the noise figure monotonically reduces with increase of frequency according to (100).

Comparing (103) to (94), it is noted that the achievable noise figure for an electrically small dipole antenna is typically higher than that of an electrically small loops due to the fact high-Q resonant matching components, i.e. inductors are missing. Yet a low noise figure can still be achieved over a broadband through the active direct matching if the transistor gate cutoff frequency and the transistor transition frequency are both higher than the transition frequency of the antenna. One advantage of using electrically small dipole antennas versus that of electrically small loops is that the noise figure worsens at the lower frequency at a slower speed (f^2 vs. f^4), because the antenna resistance in dipole antennas decreases according to the square of the frequency instead of the 4^{th} power in loop antennas, as evidenced by (2). The antenna efficiency for an unmatched electrically small dipole is generally higher than that of an electrically small loop at the same dimension which may contribute to an overall lower noise figure for dipole based receivers.

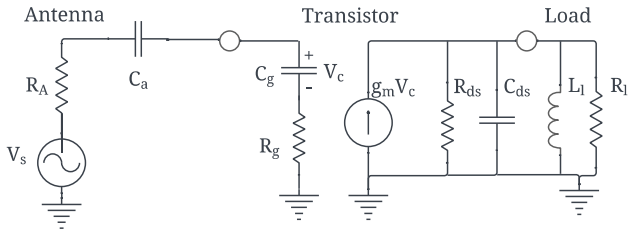

FIGURE 8. Active direct matching of an electrically small dipole antenna to a transistor.

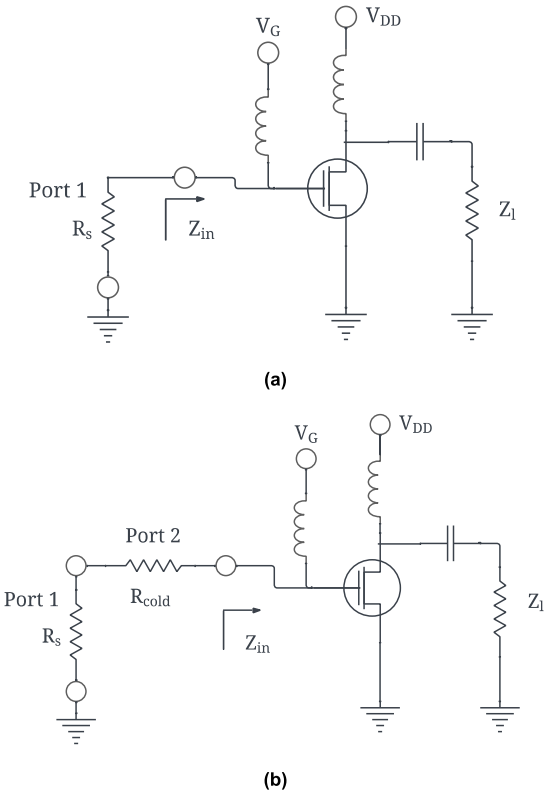

FIGURE 9. Schematic of gate parameter extraction from a FET. (a) Directly observing the input impedance (b) Extracting the gate resistance from the contributed noise figure to a cold resistor.

VII. RECEIVER DESIGN EXAMPLES

In this section, we will study the noise matching options of two electrically small antennas with HRL T3 GaN transistor models. The T3 GaN is an enhanced mode HEMT technology with a 40nm gate length and it has a transition frequency greater than 200GHz, i.e., $f_t > 200GHz$. The antennas are an electrically small loop and an electrically small dipole, both are with a maximum dimension of 24cm corresponding to ka = 1/4 at 100MHz.

A. CHARACTERIZING THE NOISE PARAMETERS OF THE TRANSISTOR

From the above analyses, it is concluded that the noise figure of the receiver is predominately determined by the ratio between the quality factor of the gate and the antenna's radiation quality factor. Therefore, to gain a better insight of

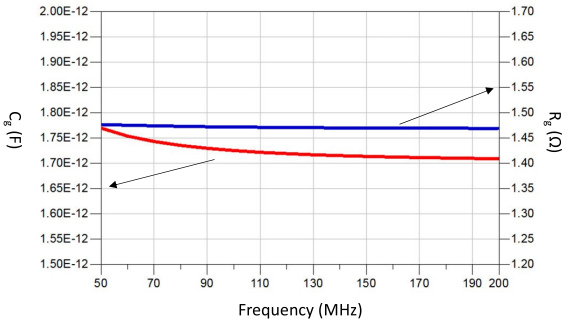

FIGURE 10. Extracted gate resistance and capacitance from the S-parameter simulation.

the transistor noise performance analytically, one may derive parameters such as R_g and C_g of the transistor from the foundry provided transistor model. Ideally the gate capacitance and resistance of a transistor can be derived as the real and imaginary part of the measured input impedance at the intended operating biasing conditions if the transistor behaves as a unidirectional device, as shown in Fig.9(a). In practice, however, the feedback of the transistor introduced by the Miller capacitance coupled with the high gain of transistor can alter the resistance reading significantly. One could exclude the active feedback effects by measuring the gate resistance at the condition of $V_{ds} = 0$ yet the gate resistance may not correspond to the gate resistance at the biased condition exactly. In this work, we measure the capacitance through the impedance measurement as shown in Fig.9(a) with $V_{ds} = 0$ while measuring the gate resistance by adding a second port of cold resistor in series with the input port and the gate and observing the noise figure from the input port (port 1) to port 2 as shown in Fig.9(b). The following equations are then used to extract the gate capacitance and resistance respectively,

$$C_g = \frac{1}{[\omega \cdot imag\,(Z_{in})]} \tag{106}$$

$$R_g = (NF - 1) \cdot R_s \tag{107}$$

S-parameter simulations are carried out for a 12 × 100um FET device from the HRL T3 GaN model library. The device is source grounded and biased with a gate voltage of 0V and drain voltage of 6V. The output load is 15Ohm. The extracted gate resistance and capacitance from 50MHz to 200MHz are shown in Fig.10, which shows a gate resistance of 1.47Ω and capacitance of 0.73pF approximately.

The quality factor of the gate is obtained using (33), which is plotted in Fig.11. The gate quality factor is 627 at 100MHz, which corresponds to a gate cutoff frequency of $\omega_{gc} = 2\,\pi \times 148GHz$. The simulated transconductance under the biasing condition ($V_{gs} = 0$, $V_{ds} = 6V$) is $g_m = 0.67$, which gives the transition frequency $\omega_T = g_m/C_g = 2\pi \times 146GHz$. One may also measure the channel resistance R_{ch} through simulating the drain current noise. By putting the gate in open circuit and measure the output noise power to a cold resistor, the channel

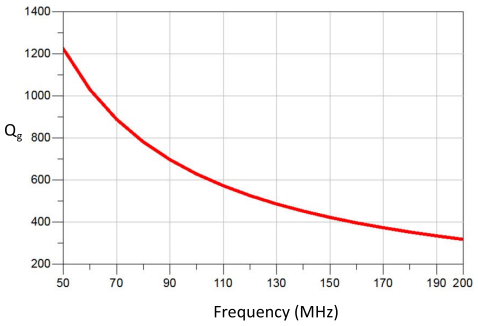

FIGURE 11. Extracted quality factor of the gate from the S-parameter simulation.

resistance under the same biasing condition is derived to be $R_{ch} = 2.7\ \Omega$. The device form factor γ is then obtained as,

$$r = \frac{1}{R_{ch} g_m} = 0.55 \tag{108}$$

B. EXAMPLE OF A RECEIVER WITH AN ELECTRICALLY SMALL LOOP ANTENNA

A planar electrically small loop is designed with 20um thick copper traces on Rogers 5870 substrate that has a dielectric constant of 2.33 and dielectric thickness of 1mm. The dimension of the antenna is shown in Fig.12(a), with a radius of 12cm (ka = 1/4 @100MHz) and the width of the trace is 2.4cm. The S-parameter of the loop is simulated in ADS Momentum which is based on method of moments (MoM). Chu's circuit model as shown in the middle column of Fig.1(b) is extracted with the following parameters,

$$R_r = 10.5\Omega, \quad L_0 = 400nH, \ C_0 = 1.6pF \tag{109}$$

The simulated antenna radiation efficiency is 90% at 100MHz and an additional Ohmic resistance of 0.056Ω is added in series to the antenna port. Fig.12(b) and (c) show the comparison between the amplitudes and phases of S-parameters obtained from MoM simulation and from the circuit model and very good agreements are observed from 20MHz to 120MHz. Parameters in (109) gives a transformed antenna resistance $R_a = 0.85\Omega$ and $L_a = 535nH$ (assuming 100MHz center frequency), obtained from (2). Antenna quality factor is yielded to be 375 at 100MHz including the Ohmic resistance from (3). The transition frequency of the antenna is thus 721MHz from (4).

The equivalent circuit of the loop antenna is now connected to a differential LNA designed with the HRL T3 GaN transistors for simulation of noise figure that is defined from the wave port to the output of the LNA, as shown in Fig.13.

Note that in the design a source degenerating inductor of $L_d = 4nH$ per 12×100um transistor is used for stabilization. A series LR circuit is also added at the output for impedance matching and additional stabilization purposes so that the stability factor is yielded to be greater than 1 through all the frequencies.

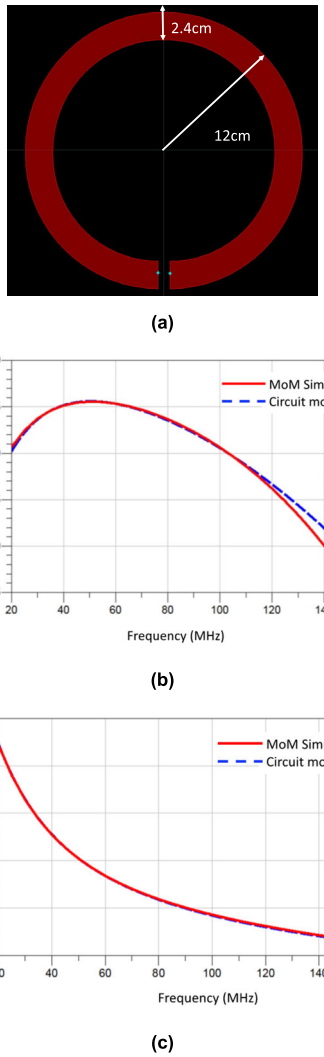

FIGURE 12. Layout of the planar loop antenna with a radius of 12cm (ka = 1/4@100MHz) (b) magnitude of S-parameters obtained from ADS Momentum and the circuit model extracted (c) phase of S-parameters obtained from ADS Momentum and the circuit model extracted.

The first noise matching option is assuming the use of a matching capacitor C_m to resonate with the inductance of the antenna L_a at 100MHz. The value of C_m is adjusted for different device peripheries. Two types of transistors are used for simulation study, one is with a periphery of 6×50um and the second one is 12×100um. The total capacitance required to resonate with the antenna is approximately 4.85pF which gives two capacitance ratios for these two cases at 53 and 13.3 respectively. The simulated transducer gains and stability factors are plotted in Fig.14(a) and (b). The stabilization circuits as shown in Fig.13 must be used to obtain a stability factor greater than 1 through the entire frequency of consideration. The transducer gains shown in Fig.14(a), therefore, are not corresponding to the theoretical transducer gain presented in the previous discussions. The yielded maximum transducer gains are similar for both cases

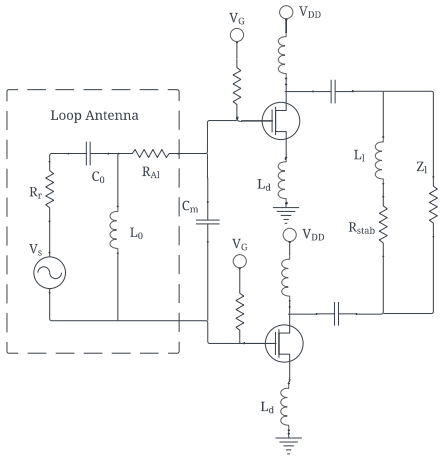

FIGURE 13. Circuit simulation setup for the receiver with an electrically small loop antenna.

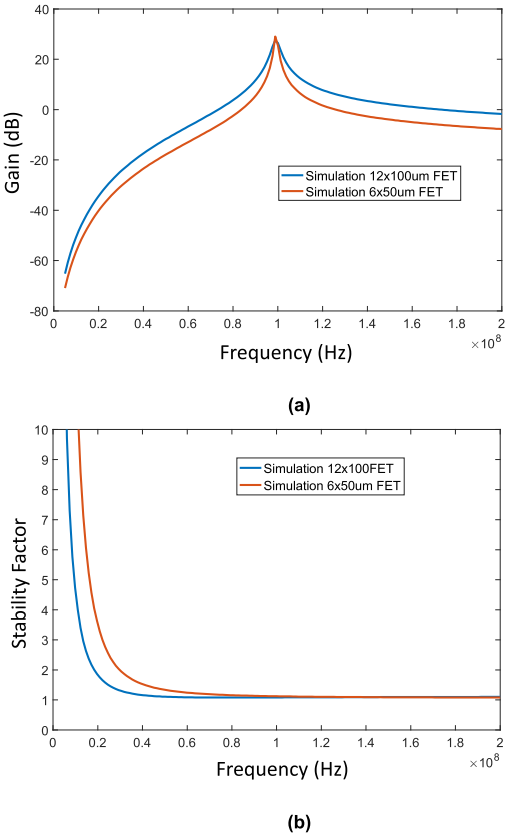

FIGURE 14. Simulated results for electrically small loop receivers under resonant match with transistors in two different peripheries (a) transducer gain (b) stability factor.

while the transistor with the larger periphery offers a slightly wider transducer gain bandwidth.

The noise figure behaviors, however, are found not altered by those stabilization circuits as shown in Fig.15. The simulated noise figure with the 6 × 50um FET device is of much narrower band and its 3dB noise figure bandwidth is 20MHz vs. 40MHz when a 12 × 100um FET device is used. The

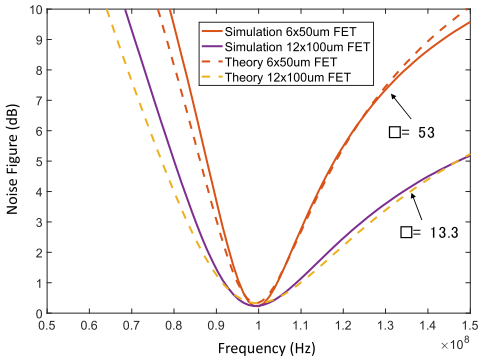

FIGURE 15. Simulated noise figures for electrically small loop receivers under resonant match with transistors in two different peripheries.

theoretical prediction based on (84) is also plotted against the simulation results which shows very good agreement. The DC power consumption for this case is 0.94W and 3.77w respectively.

The second noise matching option is active direct match, which is to eliminate the matching capacitor completely and rely solely on the parasitic capacitance of the transistors for resonance match. The required transistor peripheries are therefore significantly greater than before. One can shunt a number of largest single transistors (12×100um) in the model library to create such a "super" transistor. The simulated gains and stability factors of the amplifiers with 20, 10 and 5 transistors are shown in Fig.16. It is noted that a broadband gain is obtained with this setting and the stability factors in all cases are above 1, thanks to the stabilization circuits. The peak gain frequency is shifted to lower when a larger number of transistors are used due to the higher parasitic capacitance.

Simulated noise figure results show a low pass type of noise figure characteristics as shown in Fig.17 and the noise figures beyond certain cutoff frequency remain flat as discussed in the theory. In particular, the agreement with the theoretical prediction of noise figures in (90) is very good, as shown in Fig.17. It is also evident that a lower cutoff frequency and a wider bandwidth can be realized with a large number of transistors in parallel. 20 transistors have brought down the 3dB noise figure cutoff to 68MHz. Since each transistor has a DC biasing current of 314mA. The total DC power consumption for this case is thus $0.314 \times 2 \times 20 \times 6 = 75$Watt. The power consumption, however, can be significantly reduced when low voltage transistors such as InP or CMOS transistors are used.

C. EXAMPLE OF A RECEIVER WITH AN ELECTRICALLY SMALL DIPOLE ANTENNA

A planar electrically small dipole is designed with 20um thick copper traces on Rogers 5870 substrate that has a dielectric constant of 2.33 and dielectric thickness of 1mm. The dimension of the antenna is a bowtie shown in Fig.18(a), with a radius of 12cm (ka = 1/4 @100MHz) and the opening angle of 90 degrees. The S-parameter of the loop is simulated

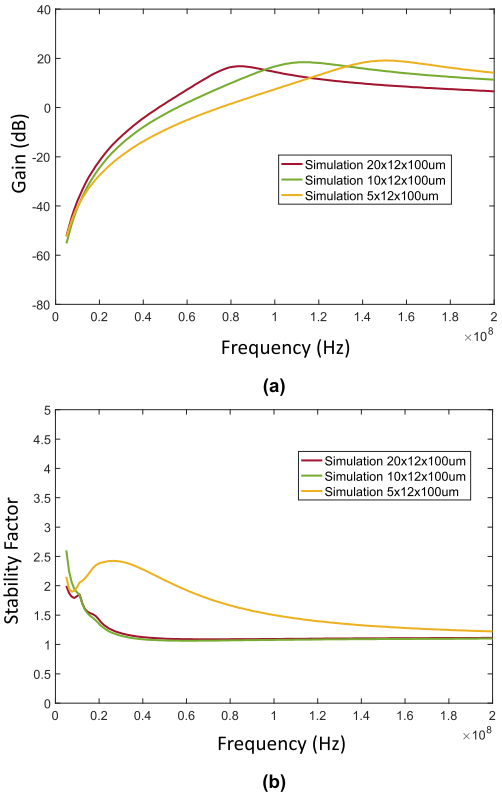

FIGURE 16. Simulated results for electrically small loop receivers under active direct match with transistors in three different peripheries (a) transducer gain (b) stability factor.

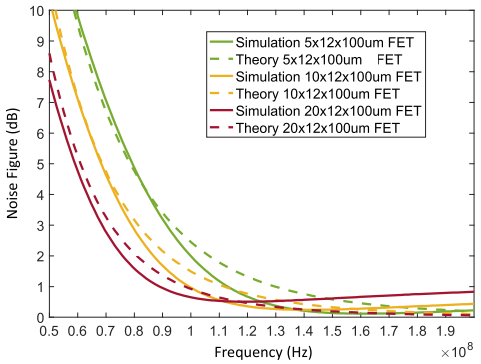

FIGURE 17. Simulated noise figures for electrically small loop receivers under active direct match with transistors in three different peripheries.

in ADS Momentum which is based on method of moments (MoM). Chu's circuit model as shown in the middle column of Fig.1(a) is extracted with the following parameters,

$$R_r = 495\Omega, \quad L_0 = 35nH, \; C_0 = 3pF \tag{110}$$

The simulated antenna radiation efficiency is almost 100% over the interested frequency and Ohmic resistance is thus ignored in this case. Fig.18(b) and (c) show the comparison between the amplitudes and phases of S-parameters obtained from MoM simulation and from the circuit model and very good agreements are observed from 20MHz to 120MHz.

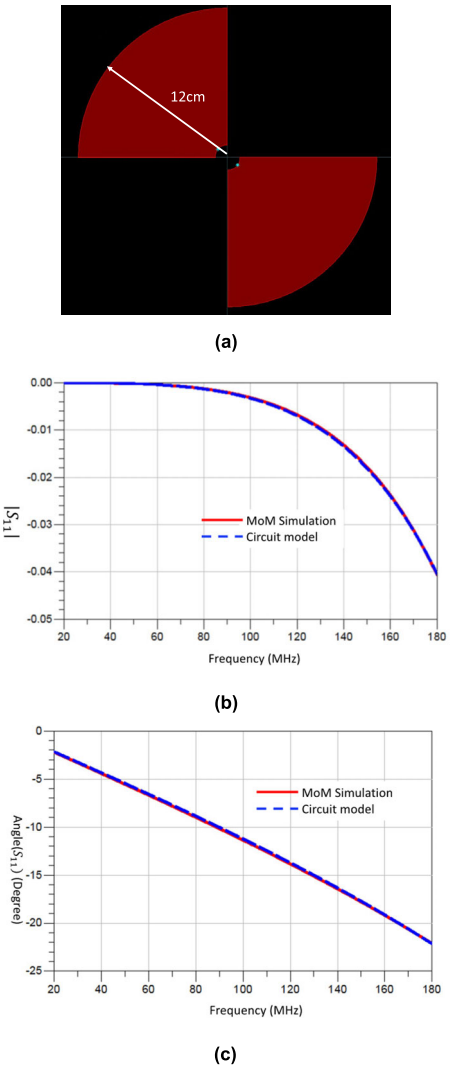

FIGURE 18. (a) Layout of the planar dipole antenna with a radius of 12cm (ka = 1/4 @100MHz) (b) magnitude of S-parameters obtained from ADS Momentum and the circuit model extracted (c) phase of S-parameters obtained from ADS Momentum and the circuit model extracted.

Parameters in (110) gives a transformed antenna resistance $R_a = 0.98\Omega$ and $C_a = 3.13pF$ (assuming 100MHz center frequency), obtained from (2). Antenna quality factor is yielded to be 543 at 100MHz. The transition frequency of the antenna is thus 816MHz from (4). The equivalent circuit of the dipole antenna is now connected to a differential LNA designed with the HRL T3 GaN transistors for simulation of noise figure that is defined from the wave port to the output of the LNA, as shown in Fig.19. A shunt inductor Lm is used for resonance with the dipole in a conventional setup and it is removed for direct active matching. Similar to the loop antenna case, a source degenerating inductor of $L_d = 4nH$ per 12×100um transistor is used for stabilization. A series LR circuit is also added at the output for impedance matching and additional stabilization purposes so that the stability factor is yielded to be greater than 1 through all the frequencies.

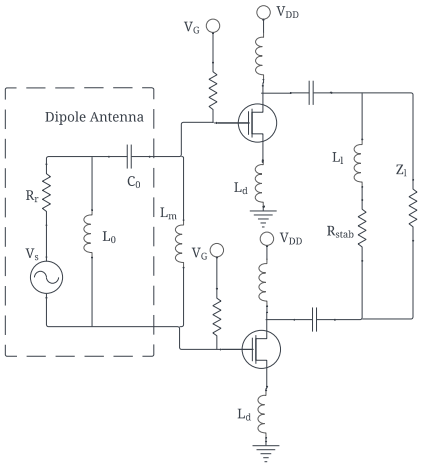

FIGURE 19. Circuit simulation setup for the receiver with an electrically small dipole antenna.

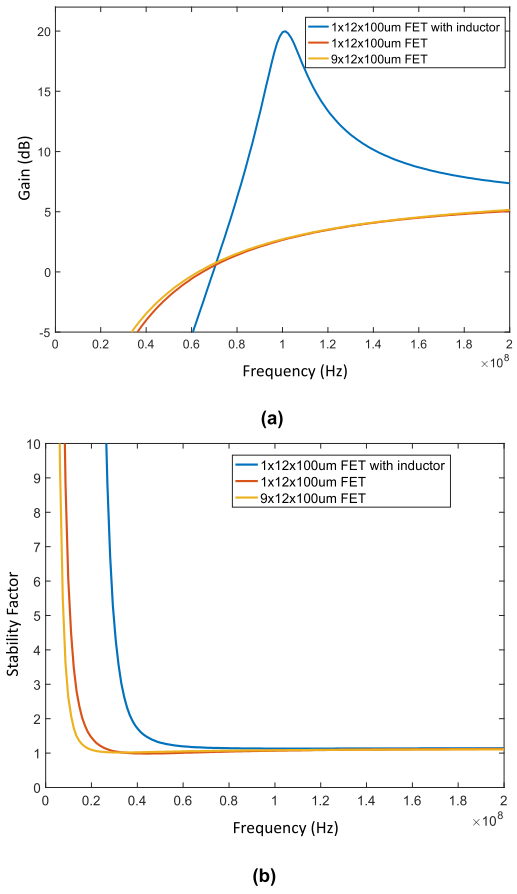

FIGURE 20. Simulated results for electrically small dipole receivers under resonance matching and active direct match with transistors in two different peripheries (a) transducer gain (b) stability factor.

Three matching cases are studied. The first case is to use the shunt inductor L_m to resonate with both the dipole and the gate capacitance of the transistor. With a 12 × 100um FET in each amplifier, the inductance is 700nH and the quality factor of 60 is assumed, which is consistent to those lumped

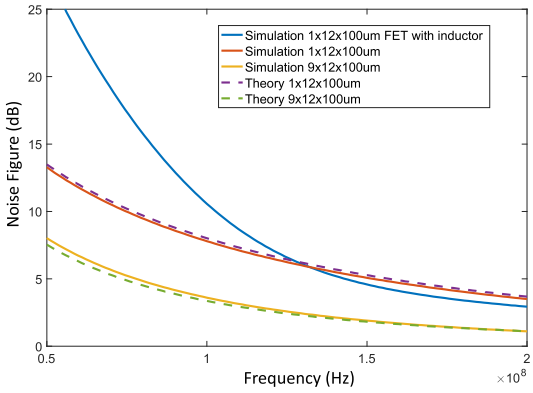

FIGURE 21. Simulated noise figures for electrically small dipole receivers under resonance matching and active direct match with transistors in two different peripheries.

inductors from Murata at this frequency range. When the antenna is directly connected to transistors, different peripheries can also be used. We will use 1 or 9 largest single transistors (12 × 100um) in the model library in shunt for the study. The 9-transistor case offers a total gate capacitance close to that of the antenna capacitance ($\beta \approx 1$) and 1 transistor case gives $\beta = 8.6$. The simulated gains and stability factors amplifiers for all three cases are shown in Fig.20. It is noted that the resonance match case results in a high transducer gain of about 20dB at around 100MHz as expected and both active direct matching cases are very similar, with mild, broadband gains obtained with this setting. The stability factors in all cases are above 1 due to the use of stabilization circuits.

Fig.21 show the simulated noise figures for all three cases. The resonance match case shows the worst noise figure at 100MHz in spite of its high transducer gain because of the noise added by the matching inductor. For active direct matching, the 9-transistor case shows a much superior noise performance than the 1-transistor case as it is close to the optimum match condition defined in (101). A larger than 9 number of transistors could also be used but with very little or no improvement in noise figure due to a poorer transducer gain. The simulated noise figures for both cases, however, are in very good agreements with the theory described in (100) as shown in Fig.21.

VIII. CONCLUSION

A general theory regarding the noise matching performance of receivers with electrically small antennas (ESAs) has been proposed based on theoretical analyses and discussions, and circuit simulations with practical device models from a state-of-the art semiconductor technology. The theory considers all the noise sources and their interplay. The noise performance of the receiver is formulated as functions of the antenna's radiation quality factor and the key parameters of the transistor technology such as gate resistance, gate cutoff frequency and transistor transition frequency. Two receiver examples, one with electrically small dipole and the other with electrically small loop have been studied jointly with

state-of-the art GaN transistor models. It is concluded that conventional resonance impedance match strategy of electrically small antennas does neither offer the best noise figure nor a broad bandwidth. An optimized joint antenna and LNA design or active direct matching method achieves better noise figure and broader noise matching bandwidth, at the price of increased transistor periphery. In particular, the bandwidth of such low noise matching can be orders of magnitude wider than the antenna's conjugate impedance matching bandwidth that is defined by Harrington-Chu's limit.

ACKNOWLEDGMENT

The views and conclusions contained herein are those of the authors and should not be interpreted as necessarily representing the official policies, either expressed or implied, of ODNI, IARPA, or the U.S. Government. The U.S. Government is authorized to reproduce and distribute reprints for governmental purposes notwithstanding any copyright annotation therein.

REFERENCES

[1] R. A. Burberry, "Electrically small antennas: A review," in *Proc. IEE Colloq. Electrically Small Antennas*, London, U.K., 1990, pp. 1.
[2] R. C. Hansen, *Electrically Small, Superdirective, and Superconducting Antennas*, 1st ed. Hoboken, NJ, USA: Wiley, 2006.
[3] R. Hansen and R. Collin, *Small Antenna Handbook*, 1st ed. Hoboken, NJ, USA: Wiley, 2011.
[4] S. R. Best, "A discussion on the properties of electrically small self-resonant wire antennas," *IEEE Antennas Propag. Mag.*, vol. 46, no. 6, pp. 9–22, Dec. 2004.
[5] S. R. Best, "The radiation properties of electrically small folded spherical helix antennas," *IEEE Trans. Antennas Propag.*, vol. 52, no. 4, pp. 953–960, Apr. 2004.
[6] S. Lim, R. L. Rogers, and H. Ling, "A tunable electrically small antenna for ground wave transmission," *IEEE Trans. Antennas Propag.*, vol. 54, no. 2, pp. 417–421, Feb. 2006.
[7] S. R. Best, "Electrically small resonant planar antennas: Optimizing the quality factor and bandwidth," *IEEE Antennas Propag. Mag.*, vol. 57, no. 3, pp. 38–47, Jun. 2015.
[8] D. F. Sievenpiper, D. C. Dawson, M. M. Jacob, T. Kanar, S. Kim, J. Long, and R. G. Quarfoth, "Experimental validation of performance limits and design guidelines for small antennas," *IEEE Trans. Antennas Propag.*, vol. 60, no. 1, pp. 8–19, Jan. 2012.
[9] C. Pfeiffer, "Fundamental efficiency limits for small metallic antennas," *IEEE Trans. Antennas Propag.*, vol. 65, no. 4, pp. 1642–1650, Apr. 2017.
[10] F. T. Dagefu, J. Choi, B. M. Sadler, and K. Sarabandi, "A survey of small, low-frequency antennas: Recent designs, practical challenges, and research directions," *IEEE Antennas Propag. Mag.*, vol. 65, no. 1, pp. 14–26, Feb. 2023.
[11] H. A. Wheeler, "Fundamental limitations of small antennas," *Proc. IRE*, vol. 35, no. 12, pp. 1479–1484, Dec. 1947.
[12] L. J. Chu, "Physical limitations of omni-directional antennas," *J. Appl. Phys.*, vol. 19, no. 12, pp. 1163–1175, Dec. 1948.
[13] M. Gustafsson, C. Sohl, and G. Kristensson, "Physical limitations on antennas of arbitrary shape," *Proc. Roy. Soc. A, Math., Phys. Eng. Sci.*, vol. 463, no. 2086, pp. 2589–2607, Oct. 2007.
[14] J. Copeland, W. Robertson, and R. Verstraete, "Antennafier arrays," *IEEE Trans. Antennas Propag.*, vol. AP-12, no. 2, pp. 227–233, Mar. 1964.
[15] H. H. Meinke, "Active antennas," *Nachrichtentechnische Zeitschrift*, vol. 19, pp. 697–705, Dec. 1966.
[16] G. Flachenecker, "Active receiving antennas," *De Ingenieur*, vol. 84, pp. 74–80, Jun. 1972.
[17] J. P. Daniel, G. Dubost, and J. Rospars, "Transistor-fed thick folded dipole with large bandwidth at reception," *Electron. Lett.*, vol. 11, pp. 90–92, Feb. 1975.
[18] M. E. Pedinoff, "The negative-conductance slot amplifier," *IEEE Trans. Microw. Theory Techn.*, vol. MTT-9, no. 6, pp. 557–566, Nov. 1961.
[19] H. H. Meinke, "Tunnel diodes integrated with microwave antenna systems," *Radio Elect. Engineer*, vol. 31, pp. 76–80, Feb. 1966.
[20] A. D. Frost, "Parametric-amplifier antenna," *Proc. IRE*, vol. 48, pp. 1163–1164, Jun. 1960.
[21] L. H. Rorden, "A study of low-noise broadband VLF receiving techniques," U.S. Naval Res. Laboratories, Washington, DC, USA, Final Rep., AD0660050, Sep. 1965.
[22] A. J. Bahr, "On the use of active coupling networks with electrically small receiving antennas," *IEEE Trans. Antennas Propag.*, vol. AP-25, pp. 841–8545, no. 6, Nov. 1977.
[23] S. E. Sussman-Fort and R. M. Rudish, "Non-foster impedance matching of electrically-small antennas," *IEEE Trans. Antennas Propag.*, vol. 57, no. 8, pp. 2230–2241, Aug. 2009.
[24] M. M. Jacob and D. F. Sievenpiper, "Gain and noise analysis of non-foster matched antennas," *IEEE Trans. Antennas Propag.*, vol. 64, no. 12, pp. 4993–5004, Dec. 2016.
[25] S. R. Best, "Optimizing the receiving properties of electrically small HF antennas," *URSI Radio Sci. Bull.*, vol. 2016, no. 359, pp. 13–29, Dec. 2016.
[26] K. Sarabandi and M. Rao, "Bandwidth and SNR of small receiving antennas: To match or not to match," *IEEE Trans. Antennas Propag.*, vol. 71, no. 1, pp. 99–104, Jan. 2023.
[27] P. Loghmannia and M. Manteghi, "Broadband parametric impedance matching for small antennas using the bode-fano limit: Improving on Chu's limit for loaded small antennas," *IEEE Antennas Propag. Mag.*, vol. 64, no. 5, pp. 55–68, Oct. 2022.
[28] A. Mekawy, H. Li, Y. Radi, and A. Alù, "Parametric enhancement of radiation from electrically small antennas," *Phys. Rev. Appl.*, vol. 15, no. 5, May 2021, Art. no. 054063.
[29] S. R. Best, "Realized noise figure of the general receiving antenna," *IEEE Antennas Wireless Propag. Lett.*, vol. 12, pp. 702–705, 2013.
[30] C. A. Balanis, *Antenna Theory: Analysis and Design*, 4th ed. Hoboken, NJ, USA: Wiley, 2016.
[31] W. Gu, K. Luong, Z. Yao, H. Cui, and Y. E. Wang, "Ferromagnetic resonance-enhanced electrically small antennas," *IEEE Trans. Antennas Propag.*, vol. 69, no. 12, pp. 8304–8314, Dec. 2021.
[32] D. Pozar, *Microwave Engineering*, 3rd ed. Hoboken, NJ, USA: Wiley, 2015.
[33] A. Grebennikov, *RF and Microwave Transmitter Design*, 1st ed. Hoboken, NJ, USA: Wiley, 2011.

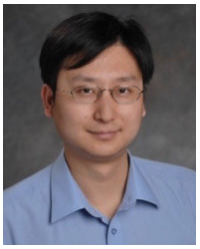

YUANXUN ETHAN WANG (Fellow, IEEE) received the B.S. degree in electrical engineering from the University of Science and Technology of China (USTC), Hefei, China, in 1993, and the M.S. and Ph.D. degrees in electrical engineering from The University of Texas at Austin, in 1996 and 1999, respectively. He became an Assistant Professor with the Electrical and Computer Engineering Department, University of California, Los Angeles (UCLA), in November 2002, where he is currently a Full Professor. He is also the Director of the Digital Microwave Laboratory, Electrical and Computer Engineering Department, UCLA. He has published more than 200 journals and conference papers. His expertise ranges from microwave systems to devices. His research blends digital technologies and time-varying concepts into RF design, which often leads to novel devices with performances beyond the conventional bound.

He is an IEEE Fellow with the Microwave Theory and Techniques (MTT) Society. He was a co-recipient of the first place Best Student Paper Award at the International Microwave Symposium, in 2017, and the Best Student Paper Award at the GOMAC Tech Symposium, in 2017. He has served as an Associate Editor for IEEE TRANSACTIONS ON ANTENNAS AND PROPAGATION.